Inorganic Chemistry

Article

pubs.acs.org/IC

Cooperative Anion Recognition in Copper(II) and Zinc(II) Complexes with a Ditopic Tripodal Ligand Containing a Urea Group

Israel Carreira-Barral, Teresa Rodríguez-Blas, Carlos Platas-Iglesias, Andrés de Blas, and David Esteban-Gómez*

Departamento de Química Fundamental, Universidade da Coruña, Campus da Zapateira, Rúa da Fraga 10, 15008 A Coruña, Spain

Supporting Information

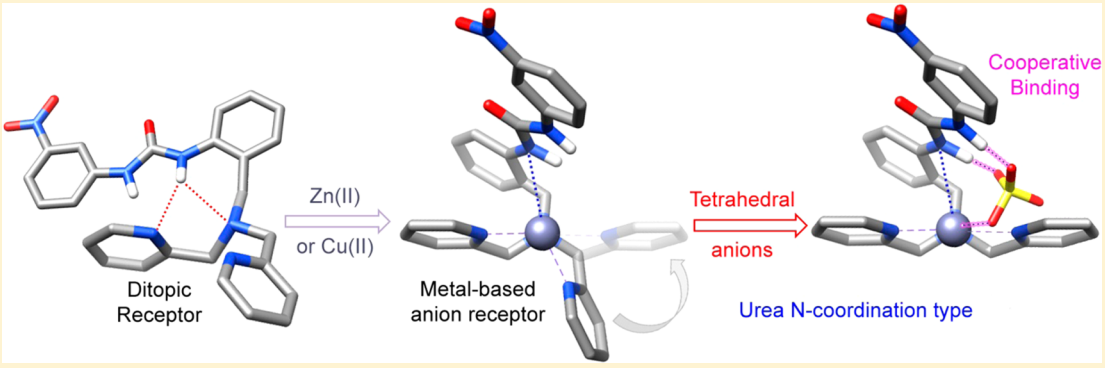

ABSTRACT: The ability of Cu^{II} and Zn^{II} complexes of the ditopic receptor H_2L [1-(2-((bis(pyridin-2-ylmethyl)amino)-methyl)phenyl)-3-(3-nitrophenyl)urea] for anion recognition is reported. In the presence of weakly coordinating anions such as ClO_4^-, the urea group binds to the metal ion (Cu^{II} or Zn^{II}) through one of its nitrogen atoms. The study of the interaction of the metal complexes with a variety of anions in DMSO shows that SO_4^{2-} and Cl^- bind to the complexes through a cooperative binding involving simultaneous coordination to the metal ion and different hydrogen-bonding interactions with the urea moiety, depending on the shape and size of the anion. On the contrary, single crystal X-ray diffraction studies show that anions such as NO_3^- and $PhCO_2^-$ form 1:2 complexes (metal/anion) where one of the anions coordinates to the metal center and the second one is involved in hydrogen-bonding interaction with the urea group, which is projected away from the metal ion. Spectrophotometric titrations performed for the Cu^{II} complex indicate that this system is able to bind a wide range of anions with an affinity sequence: $MeCO_2^- \sim Cl^-$ ($\log K_{11} > 7$) > NO_2^- > $H_2PO_4^- \sim Br^-$ > HSO_4^- > NO_3^- ($\log K_{11} < 2$). In contrast to this, the free ligand gives much weaker interactions with these anions. In the presence of basic anions such as $MeCO_2^-$ or F^-, competitive processes associated with the deprotonation of the coordinated N−H group of the urea moiety take place. Thus, N-coordination of the urea unit to the metal ion increases the acidity of one of its N−H groups. DFT calculations performed in DMSO solution are in agreement with both an anion-hydrogen bonding interaction and an anion−metal ion coordination collaborating in the stabilization of the metal salt complexes with tetrahedral anions.

INTRODUCTION

Selective anion recognition using organic receptors has been the subject of intense research efforts in the last 15 years due to their fundamental role in a wide range of chemical, biological, and environmental processes.[1] The design of receptors with improved anion recognition properties is not an easy task, and different strategies have been developed over the years for this purpose. Factors such as the charge to radius ratio of the target anion, as well as its geometry and its protonation state, must be taken into account.[2] Traditionally, anion receptors comprised organic frameworks containing suitable hydrogen-bonding donor functions.[3,4] More recently, organic anion receptors taking advantage of halogen-bonding interactions have also been developed.[5] A third approach to anion receptors is the use of dynamically self-assembled hosts formed through reversible bond formation.[6] An alternative to the use of organic scaffolds exploits the anion binding properties of coordinatively unsaturated coordination compounds.[7] The use of ditopic receptors, which contain covalently linked sites for the complexation of both a cation and an anion in a single molecule, represents another attractive alternative.[8] The binding of the cation increases the affinity of the receptor for the anion, thereby enhancing the affinity toward different anions that normally coordinate poorly with monotopic molecular receptors. In order to maximize the cooperative effect, the combined cation- and anion-recognition domains have to be close enough into a preorganized platform.

Complexes of transition and post-transition metal ions with polypyridyl ligands such as di(2-picolyl)amine (dpa) are still

Received: November 15, 2013
Published: February 17, 2014

 © 2014 American Chemical Society dx.doi.org/10.1021/ic402855r | Inorg. Chem. 2014, 53, 2554−2568

receiving much attention for the design of systems for a number of biological, catalytic, and sensing applications.[9] For instance, Cu^{II} and Zn^{II} complexes with dpa[10] and different *N*-substituted derivatives have been widely investigated.[11] These complexes are often coordinatively unsaturated, and therefore, they possess anion recognition properties that have been exploited for the design of luminescent sensors for different anions.[12]

Urea-based receptors are known to be suitable for anion recognition, as they can establish hydrogen-bonding interactions with different anions,[13] in particular Y-shape ones.[14] Ditopic receptors containing urea- or thiourea units and metal binding moieties have been developed for different purposes (i.e., metal controlled assembly of anion receptors,[15] extraction of ion-pairs from aqueous media,[16] ion-pair sensing,[17] or anion recognition via cooperative binding through anion coordination to the metal ion and hydrogen-bonding interactions).[18] In view of this, we envisaged that ditopic receptors containing a urea moiety and a dpa unit might be useful for the recognition of different anions. Thus, in this paper we report the ability of the Cu^{II} or Zn^{II} complexes of the ditopic receptor H_2L (Scheme 1)

Scheme 1. Synthesis of H_2L and Numbering Scheme used for NMR Spectral Assignment

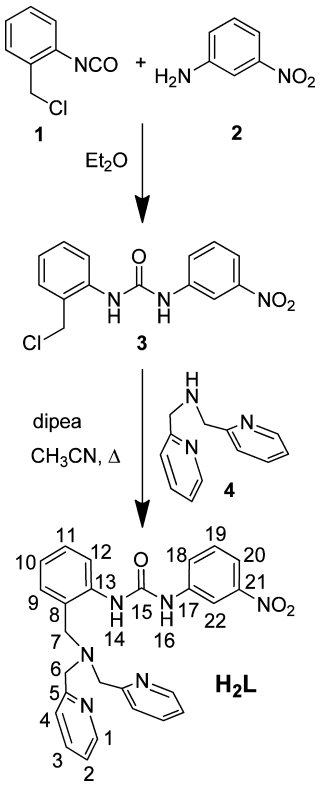

for anion recognition. In particular, the affinity of the $[Cu(H_2L)]^{2+}$ complex toward different anions (F^-, NO_3^-, HSO_4^-, $H_2PO_4^-$, NO_2^-, Cl^-, Br^-, $MeCO_2^-$, and $PhCO_2^-$) has been investigated by using electronic absorption spectroscopy. A structural analysis of anion recognition with the Zn^{II} analogue in solution (NMR spectroscopy supported by DFT calculations) is also reported.

EXPERIMENTAL AND COMPUTATIONAL SECTION

Materials. 1-(Chloromethyl)-2-isocyanatobenzene (**1**), 3-nitroaniline (**2**), and bis(pyridin-2-ylmethyl)amine (**4**) were obtained from commercial sources. Solvents were of reagent grade and used without further purification.

Caution: *Although we have experienced no difficulties with the perchlorate salts, these should be regarded as potentially explosive and handled with care. To avoid the formation of peroxides due to contact with air, reflux of ether solutions was carried out under Ar.*

General Methods. Elemental analyses were carried out on a ThermoQuest Flash EA 1112 elemental analyzer. ESI-TOF mass spectra were recorded from MeOH/H_2O/MeCN or MeOH solutions using a LC-Q-q-TOF Applied Biosystems QSTAR Elite spectrometer in the positive mode. IR spectra were recorded using a Bruker Vector 22 spectrophotometer equipped with a Golden Gate attenuated total reflectance (ATR) accessory (Specac). ^1H and ^{13}C NMR spectra were recorded at 25 °C on Bruker Avance 300 and Bruker Avance 500 spectrometers, and spectral assignments were based in part on 2D COSY, HSQC, and HMBC experiments. UV/vis spectra were recorded with a Perkin-Elmer Lambda 900 spectrophotometer; those performed in solution were recorded with quartz cells (path length: 1 cm), and the cell holder was thermostatted at 25.0 °C, through circulating water. The formation of the mononuclear Cu^{II} complex was monitored by using spectrophotometric titrations at 25 °C on a 10^{-5} M solution of ligand H_2L in DMSO. Typically, aliquots of a fresh standard solution of $Cu(TfO)_2$ ($TfO^- = CF_3SO_3^-$) in the same solvent (10^{-3} M) were added and the UV/vis spectra of the samples were recorded. Anion binding studies were performed by monitoring the spectral changes of a 5×10^{-3} M solution of ligand H_2L in the presence of 1 equiv of $Cu(TfO)_2$ upon addition of the corresponding tetrabutylammonium salt (0.5 M in DMSO). Binding constants were obtained by using a simultaneous fit of the UV/vis absorption spectral changes at 7−12 selected wavelengths in the range 500−1200 nm. A minimum of 26 absorbance data points at each of these wavelengths was used, and all spectrophotometric titration curves were fitted with the HYPERQUAD program.[19]

*1-(2-(Chloromethyl)phenyl)-3-(3-nitrophenyl)urea (**3**).* A solution of 1-(chloromethyl)-2-isocyanatobenzene (**1**) (0.98 mL, 7.10 mmol) and 3-nitroaniline (**2**) (1.00 g, 7.10 mmol) in diethyl ether (50 mL) was heated to reflux under Ar atmosphere for 48 h. The precipitate formed was isolated by filtration and washed with diethyl ether (3 × 10 mL) to give 1.584 g of **3** (73%) as a light yellow solid. δ_H (solvent DMSO-d_6, 500 MHz, 298 K): 10.13 (s), 10.08 (s), 8.60 (s), 8.57 (t, ^4J = 2.1 Hz), 8.48 (s), 7.86 (m), 7.80 (m), 7.73 (m), 7.58−7.53 (m), 7.44 (dd, ^3J = 7.7 Hz, ^4J = 1.5 Hz), 7.35−7.31 (m), 7.24 (m), 7.09 (m), 7.03 (m), 4.88 (s), 4.55 (s). δ_C (solvent DMSO-d_6, 125.8 MHz, 298 K): 152.8, 152.7, 148.2, 148.2, 141.5, 141.2, 137.1, 136.9, 131.8, 130.7, 130.2, 130.1, 129.3, 128.3, 128.1, 127.5, 124.1, 124.0, 123.7, 122.9, 122.8, 121.6, 116.3, 116.1, 111.9, 61.0, 43.5. MS-ESI$^+$, *m*/*z* (%BPI): [**3** + H]$^+$, 306.1 (69.5%); [**3** − Cl]$^+$, 270.1 (100%). Elem. Anal. Calcd for $C_{14}H_{12}ClN_3O_3$: C, 55.0; H, 4.0; N, 13.7%. Found: C, 54.9; H, 3.6; N, 13.4%. IR: 3291 ν(N−H), 3096 ν(C−H), 1651 ν(C═O), 1594 ν(C═C), 1561 δ(C−N−H), 1522 $\nu_a(NO_2)$, 1346 $\nu_s(NO_2)$, 687 ν(C−Cl) cm^{-1}.

*1-(2-((Bis(pyridin-2-ylmethyl)amino)methyl)phenyl)-3-(3-nitrophenyl)urea (**H_2L**).* A solution of compound **3** (0.819 g, 2.678 mmol), bis(pyridin-2-ylmethyl)amine (dpa) (**4**) (0.452 mL, 2.434 mmol), *N*,*N*-diisopropylethylamine (dipea) (0.848 mL, 4.868 mmol), and a catalytic amount of KI in acetonitrile (50 mL) was heated to reflux with stirring for 16 h. The resulting solution was filtered while hot and allowed to cool down to room temperature and sonicated to give a light yellow solid that was isolated by filtration and washed with acetonitrile (10 mL) and diethyl ether (10 mL) to give 0.561 g (48%) of H_2L. δ_H (solvent DMSO-d_6, 500 MHz, 298 K): 10.30 (s, 1H, H14), 9.58 (s, 1H, H16), 8.61 (m, 1H, H22), 8.49 (m, 2H, H1), 7.89 (d, 1H, H12, ^3J = 8.0 Hz), 7.86 (dd, 1H, H20, ^3J = 8.2 Hz, ^4J = 1.8 Hz), 7.80 (m, 1H, H18), 7.73 (m, 2H, H3), 7.61 (m, 1H, H19), 7.40 (m, 2H, H4), 7.29−7.22 (m, 4H, H2, H9, and H11), 6.99 (m, 1H, H10), 3.83 (s, 4H, H6), 3.75 (s, 2H, H7). δ_C (solvent DMSO-d_6, 125.8 MHz, 298 K): 157.6 C5, 152.6 C15, 148.9 C1, 148.3 C21, 141.4 C17, 138.7 C13, 137.0 C3, 130.3 C19, 130.1 C9, 127.9 C11, 126.8 C8, 124.2 C18, 123.8 C4, 122.7 C2, 122.5 C10, 120.7 C12, 116.3 C20, 112.1 C22, 58.6 C6, 56.2 C7. MS-ESI$^+$, *m*/*z* (%BPI): [H_2L + H]$^+$, 469.2 (100%).

dx.doi.org/10.1021/ic402855r | Inorg. Chem. 2014, 53, 2554−2568

Table 1. Crystal Data and Refinement Details

	Cu·L·NO_3	Cu·L·SO_4	Cu·L·Bz	Zn·L·Cl
formula	$C_{27}H_{28}CuN_8O_{10}$	$C_{26}H_{30}CuN_6O_{10}S$	$C_{40}H_{36}CuN_6O_8$	$C_{27}H_{25}Cl_5N_6O_3Zn$
MW	688.11	682.16	792.29	724.15
crystal system	triclinic	triclinic	monoclinic	triclinic
space group	$P\bar{1}$	$P\bar{1}$	$P2_1/c$	$P\bar{1}$
T/K	100(2)	100(2)	100(2)	100(2)
a/Å	9.2361(3)	8.7439(5)	9.4204(11)	9.0531(4)
b/Å	12.3680(4)	12.9521(7)	26.459(3)	12.3579(6)
c/Å	13.5847(4)	14.6569(8)	14.3146(18)	15.7312(8)
α/deg	99.696(2)	65.471(2)	90	91.820(3)
β/deg	94.596(2)	89.183(3)	95.339(8)	99.113(3)
γ/deg	106.471(2)	70.880(3)	90	106.040(3)
V/Å^3	1453.38(8)	1412.43(14)	3552.5(7)	1664.80(14)
F(000)	710	706	1644	736
Z	2	2	4	2
λ, Å (Mo Kα)	0.71073	0.71073	0.71073	0.71073
D_{calc}/g cm^{-3}	1.572	1.604	1.481	1.445
μ/mm^{-1}	0.824	0.916	0.680	1.176
θ range/deg	1.53−28.36	2.52−28.39	2.92−27.88	2.70−28.39
R_{int}	0.0447	0.0246	0.1146	0.0296
reflns measd	26362	41327	38143	22494
unique reflns	7137	7084	8447	8132
reflns obsd	4975	6697	4805	5984
GOF on F^2	1.140	1.059	1.033	1.095
R1[a]	0.0442	0.0247	0.0581	0.0579
$wR2$ (all data)[b]	0.1194	0.0672	0.1396	0.1658
largest differences peak and hole/e Å^{-3}	0.346 and −0.871	0.497 and −0.499	0.533 and −0.659	1.183 and −1.209

[a] $R1 = \sum||F_0| - |Fc||/\sum|F_0|$. [b] $wR2 = \{\sum[w(|F_0|^2 - |Fc^2|)^2]/\sum[w(F_0^4)]\}^{1/2}$.

Elem. Anal. Calcd for $C_{26}H_{24}N_6O_3 0.5H_2O$: C, 65.4; H, 5.3; N, 17.6%. Found: C, 65.8; H, 5.1; N, 17.7%. IR: 3310−3190 ν(N−H), 3130−2850 ν(C−H), 1703 ν(C═O), 1519 $\nu_a(NO_2)$, 1345 $\nu_s(NO_2)$ cm^{-1}.

General Procedure for the Preparation of [M(H_2L)Cl_2], [M(H_2L)]-(ClO_4)$_2$, [M(H_2L)(SO_4)], and [M(H_2L)(NO_3)](NO_3) (M = Cu or Zn). A solution of MCl_2 (M = Cu or Zn) or hydrated $M(NO_3)_2$ or $M(SO_4)$ (0.105 mmol, M = Cu or Zn) in methanol (2 mL) was added to a warm solution of H_2L (0.050 g, 0.105 mmol) in methanol (5 mL). The mixture was stirred at room temperature for 16 or 1 h $M(ClO_4)_2$, and the precipitate formed was isolated by filtration, washed with methanol (2 mL) and diethyl ether (2 mL), and dried under vacuum. In some cases, an additional purification step was used to remove metal salt impurities: the precipitate was dissolved in chloroform (5 mL), the solution was filtered, and the filtrate was concentrated to dryness. The solid was treated with diethyl ether (5 mL), filtered, and dried under vacuum.

Cu(H_2L)Cl_2·0.5MeOH (Cu·L·Cl). Light blue solid. Yield 0.043 g, 66%. MS-ESI$^+$, m/z (%BPI): [Cu(H_2L)Cl]$^+$, 566.1 (100%); [Cu(HL)]$^+$, 530.1 (2%). Elem. Anal. Calcd for $C_{26}H_{24}Cl_2CuN_6O_3$·0.5MeOH: C, 51.4; H, 4.2; N, 13.6%. Found: C, 51.0; H, 3.6; N, 13.2%. Λ_M (methanol, 25 °C): 76 cm^2 Ω^{-1} mol^{-1}. IR: 3330−3190 ν(N−H), 1710 ν(C═O), 1529 $\nu_a(NO_2)$, 1346 $\nu_s(NO_2)$ cm^{-1}. UV/vis diffuse reflectance spectroscopy: 675 nm.

Cu(H_2L)(ClO_4)$_2$·2H_2O·MeOH (Cu·L·ClO_4). Dark green solid. Yield 0.075 g, 90%. MS-ESI$^+$, m/z (%BPI): [Cu(H_2L)(ClO_4)]$^+$, 630.1 (1%); [Cu(HL)]$^+$, 530.1 (61%); [Cu(H_2L)]$^{2+}$, 265.6 (1%). Elem. Anal. Calcd for $C_{26}H_{24}Cl_2CuN_6O_{11}$·2$H_2$O·MeOH: C, 40.8; H, 3.7; N, 10.0%. Found: C, 40.6; H, 4.0; N, 10.5%. Λ_M (methanol, 25 °C): 164 cm^2 Ω^{-1} mol^{-1}. IR: 3350 ν(N−H), 1695 ν(C═O), 1525 $\nu_a(NO_2)$, 1349 $\nu_s(NO_2)$, 1053 $\nu_a(ClO_4)$, 619 δ_a(OClO) cm^{-1}. UV/vis diffuse reflectance spectroscopy: 634 nm.

Cu(H_2L)(NO_3)$_2$·0.5MeOH·1.5H_2O (Cu·L·NO_3). Light blue solid. Yield 0.011 g, 16%. MS-ESI$^+$, m/z (%BPI): [Cu(HL)]$^+$, 530.1 (65%); [Cu(H_2L)]$^{2+}$, 265.6 (2%). Elem. Anal. Calcd for $C_{26}H_{24}CuN_8O_9$·0.5MeOH·1.5H_2O: C, 45.5; H, 4.2; N, 16.0%. Found: C, 45.5; H, 3.5; N, 15.5%. Λ_M (methanol, 25 °C): 110 cm^2 Ω^{-1} mol^{-1} (1:1 electrolyte). IR: 3323 ν(N−H), 1708 ν(C═O), 1523 $\nu_a(NO_2)$, 1318, 1279 $\nu(NO_3)$ cm^{-1}. UV/vis diffuse reflectance spectroscopy: 652 nm [d_{xz},d_{yz} → $d_{x^2-y^2}$ ($^2B_1$→^2E)]. Slow diffusion of diethyl ether into a solution of the complex in an acetonitrile/methanol mixture gave dark blue single crystals suitable for X-ray diffraction analysis.

Cu(H_2L)(SO_4)·1.5H_2O (Cu·L·SO_4). Light blue solid. Yield 0.049 g, 71%. MS-ESI$^+$, m/z (%BPI): [Cu(HL)]$^+$, 530.1 (91%); [Cu(H_2L)]$^{2+}$, 265.6 (2%). Elem. Anal. Calcd for $C_{26}H_{24}CuN_6O_7S$·1.5H_2O: C, 47.7; H, 4.2; N, 12.8%. Found: C, 47.5; H, 3.9; N, 12.8%. Λ_M (methanol, 25 °C): 4 cm^2 Ω^{-1} mol^{-1} (nonelectrolyte). IR: 3320−3180 ν(N−H), 1711 ν(C═O), 1524 $\nu_a(NO_2)$, 1345 $\nu_s(NO_2)$, 1036, 1027 $\nu(SO_4)$ cm^{-1}. UV/vis diffuse reflectance spectroscopy: 663 nm [d_{xz},d_{yz} → $d_{x^2-y^2}$ ($^2B_1$→^2E)]. Slow evaporation of a solution of the complex in water provided dark blue single crystals suitable for X-ray diffraction analysis.

Zn(H_2L)Cl_2 (Zn·L·Cl). Light yellow solid. Yield 0.048 g, 75%. MS-ESI$^+$, m/z (%BPI): [Zn(H_2L)Cl]$^+$, 567.1 (100%); [Zn(HL)]$^+$, 531.1 (42%); [Zn(H_2L)]$^{2+}$, 266.1 (13%). Elem. Anal. Calcd for $C_{26}H_{24}Cl_2N_6O_3Zn$: C, 51.6; H, 4.0; N, 13.9%. Found: C, 51.5; H, 3.7; N, 13.8%. Λ_M (methanol, 25 °C): 68 cm^2 Ω^{-1} mol^{-1}. IR: 3313 ν(N−H), 1707 ν(C═O), 1523 $\nu_a(NO_2)$, 1348 $\nu_s(NO_2)$ cm^{-1}. δ_H (solvent DMSO-d_6, 300 MHz, 298 K): 9.08 (s, 1H, HNC═O), 8.84 (s, 2H), 8.52 (s, 1H), 7.83 (m, 3H), 7.61−7.43 (m, 7H), 7.32−7.25 (m, 2H), 7.09 (t, 1H, ^3J = 7.0 Hz), 4.00 (s, 4H, H6), 3.81 (s, 2H, H7). Slow evaporation of a solution of the complex in chloroform provided colorless single crystals suitable for X-ray diffraction analysis.

Zn(H_2L)(ClO_4)$_2$·H_2O·MeOH (Zn·L·ClO_4). Yellow solid. Yield 0.070 g, 85%. MS-ESI$^+$, m/z (%BPI): [Zn(H_2L)(ClO_4)]$^+$, 631.1 (1%); [Zn(HL)]$^+$, 531.1 (100%); [Zn(H_2L)]$^{2+}$, 266.1 (12%). Elem. Anal. Calcd for $C_{26}H_{24}Cl_2N_6O_{11}Zn$·$H_2$O·MeOH: C, 41.2; H, 3.4; N, 10.4%. Found: C, 41.4; H, 3.8; N, 10.7%. Λ_M (methanol, 25 °C): 184 cm^2 Ω^{-1} mol^{-1}. IR: 3342 ν(N−H), 1663 ν(C═O), 1524 $\nu_a(NO_2)$, 1350 $\nu_s(NO_2)$, 1054 $\nu_a(ClO_4)$, 620 δ_a(OClO) cm^{-1}. δ_H (solvent DMSO-d_6, 300 MHz, 298 K): 9.14 (s, 1H, HNC═O), 8.59 (d, 2H, ^3J = 5.9 Hz), 8.40 (s, 1H), 8.31 (s, 1H, HNC═O), 7.99 (td, 3H, ^3J = 7.6 Hz, ^4J =

dx.doi.org/10.1021/ic402855r | Inorg. Chem. 2014, 53, 2554−2568

0.9 Hz), 7.82 (m, 1H), 7.61−7.23 (m, 10H), 4.23 (d, 2H, H6A, ^2J = 16.4 Hz), 3.80 (s, 2H, H7), 3.69 (d, 2H, H6B, ^2J = 16.4 Hz).

$Zn(H_2L)(NO_3)_2$·1.5MeOH (Zn·L·NO_3). Light yellow solid. Yield 0.036 g, 48%. MS-ESI$^+$, *m*/*z* (%BPI): $[Zn(HL)]^+$, 531.1 (100%); $[Zn(H_2L)]^{2+}$, 266.1 (3%). Elem. Anal. Calcd for $C_{26}H_{24}N_8O_9Zn$·1.5MeOH: C, 46.8; H, 4.3; N, 15.9%; Found: C, 46.7; H, 3.7; N, 15.1%. Λ_M (methanol, 25 °C): 137 cm^2 Ω^{-1} mol^{-1}. IR: 3250−3160 ν(N−H), 1691 ν(C═O), 1349 $\nu_s(NO_2)$, 1293 $\nu(NO_3)$ cm^{-1}. δ_H (solvent DMSO-d_6, 300 MHz, 298 K): 9.28 (br, HNC═O), 9.17 (br, HNC═O), aromatic protons appear at low field as complicated overlapping broad signals, 4.19 (br, −CH_2−), 3.75 (br, −CH_2−).

$Zn(H_2L)(SO_4)·H_2O$ (Zn·L·SO_4). Light yellow solid. Yield 0.059 g, 86%. MS-ESI$^+$, *m*/*z* (%BPI): $[Zn(HL)]^+$, 531.1 (95%); $[Zn(H_2L)]^{2+}$, 266.1 (100%). Elem. Anal. Calcd for $C_{26}H_{24}N_6O_7SZn·H_2O$: C, 48.2; H, 4.0; N, 13.0%. Found: C, 48.2; H, 3.9; N, 12.8%. Λ_M (methanol, 25 °C): the low solubility of this complex in methanol has prevented us from determining the conductivity value for this compound. IR: 3330−3200 ν(N−H), 1711 ν(C═O), 1528 $\nu_a(NO_2)$, 1349 $\nu_s(NO_2)$, 1117 $\nu(SO_4)$ cm^{-1}. δ_H (solvent DMSO-d_6, 300 MHz, 298 K): 10.36 (br, 1H, H16), 9.76 (br, 1H, H14), 8.91 (d, 2H, ^3J = 4.5 Hz), 8.44 (s, 1H), 7.88 (t, 2H, ^3J = 7.7 Hz), 7.75 (m, 2H), 7.48−7.30 (m, 7H), 7.12 (t, 1H, ^3J = 7.4 Hz), 6.97 (t, 1H, ^3J = 7.3 Hz), 4.41 (d, 2H, H6A, ^2J = 16.0 Hz), 4.09 (s, 2H, H7), 3.92 (d, 2H, H6B, ^2J = 16.0 Hz).

X-ray Crystal Structure Determinations. Single crystals were obtained from solutions of the isolated compounds, as described above. For the benzoate complex Cu·L·Bz, dark blue single crystals were grown by slow evaporation of a solution in methanol containing equimolar amounts of H_2L and copper(II) perchlorate in the presence of an excess of tetrabutylammonium benzoate.

Three dimensional X-ray data were collected on a BRUKER-NONIUS X8 APEX KAPPA diffractometer for Cu·L·NO_3, Cu·L·SO_4, Cu·L·Bz, and Zn·L·Cl complexes. Data were corrected for Lorentz and polarization effects and for absorption by semiempirical methods[20] based on symmetry-equivalent reflections. Complex scattering factors were taken from the program SHELX97[21] running under the WinGX program system[22] as implemented on a Pentium computer. The structures were solved by Patterson methods with DIRDIF2008,[23] except that of Cu·L·SO_4, which was solved by direct methods with SHELXS-97. All structures were refined by full-matrix least-squares on F^2. For the four compounds all hydrogen atoms were included in calculated positions and refined in riding mode, except those bonded to the nitrogen atoms of the urea moiety, which were refined either freely (Cu·L·NO_3 and Cu·L·SO_4) or in riding mode but with refined distances (Zn·L·Cl and Cu·L·Bz). Finally, the hydrogen atoms of the water molecules in Cu·L·Bz were located in a difference electron-density map and all the distances fixed. The crystal structure of Cu·L·NO_3 shows positional disorder for the coordinated nitrate anion and one pyridine arm of the ligand with an occupation factor of 0.57(3) for the atoms labeled as A. For Zn·L·Cl we have cleaned up the data with SQUEEZE[24] in the last steps of the structure refinement process to avoid the problems generated by a disordered chloroform molecule sitting in a special position. Finally, refinement converged with anisotropic displacement parameters for all non-hydrogen atoms for all four crystals. Crystal data and details on data collection and refinement are summarized in Table 1.

Computational Details. All calculations presented in this work were performed employing the Gaussian 09 package (Revision B.01).[25] Full geometry optimizations of Cu^{II} and Zn^{II} complexes with the receptor H_2L were carried out in dimethyl sulfoxide solution employing DFT within the hybrid meta-GGA approximation with the TPSSh exchange-correlation functional.[26] Calculations were performed on the $[M(H_2L)(OSMe_2)_2]^{2+}$ (M = Cu, Zn) systems, which explicitly include two DMSO ligands to satisfy the octahedral coordination environment. Structure optimizations were also performed on the hydrogen sulfate adduct $[Zn(H_2L)(OSMe_2)(OS(O)_2OH)]^+$, which contains an explicit DMSO molecule and $[M(H_2L)Cl_2]$ complexes (M = Cu^{II} or Zn^{II}). Input geometries were generated from the crystallographic data of $[Zn(H_2L)Cl_2]$. For geometry optimization purposes we used the standard Ahlrichs' valence double-ξ basis set including polarization functions (SVP).[27] No symmetry constraints have been imposed during the optimizations. The stationary points found on the potential energy surfaces as a result of geometry optimizations were tested to represent energy minima rather than saddle points via frequency analysis. The default values for the integration grid (75 radial shells and 302 angular points) and the SCF energy convergence criteria (10^{-8}) were used in all calculations. Since the calculations on the $[Cu(H_2L)(OSMe_2)_2]^{2+}$ system were performed by using an unrestricted model, spin contamination[28] was assessed by a comparison of the expected difference between $S(S+1)$ for the assigned spin state ($S(S+1) = 0.75$) and the actual value of $\langle S^2\rangle$. The results obtained indicate that spin contamination is negligible [$\langle S^2\rangle - S(S+1) = 0.002$]. Throughout this work solvent effects (DMSO) were included by using the polarizable continuum model (PCM), in which the solute cavity is built as an envelope of spheres centered on atoms or atomic groups with appropriate radii. In particular, we used the integral equation formalism (IEFPCM) variant as implemented in Gaussian 09.[29]

RESULTS AND DISCUSSION

Syntheses. The synthetic strategy used for the preparation of H_2L is shown in Scheme 1. Compound **3** was prepared in good yield (73%) by reaction of commercially available precursors **1** and **2**. The ^{1}H and ^{13}C NMR spectra of **3** indicate the presence of two major isomers in solution with a 3:2 ratio, which are attributed to the (*trans, trans*) and (*trans, cis*) conformations typically adopted by *N,N′*-diarylureas.[30] *N*-Alkylation of bis(pyridin-2-ylmethyl)amine (**4**) with **3** in refluxing acetonitrile in the presence of dipea and a catalytic amount of KI gave H_2L in 48% yield. In contrast to compound **3**, H_2L exists in solution as a single isomer, presumably the (*trans, trans*) conformation.[30a]

The coordination of H_2L to Cu^{II} was monitored by spectrophotometric titrations. The UV/vis spectrum of H_2L recorded in DMSO solution shows a band at 262 nm (ε = 45600 M^{-1} cm^{-1}) that is attributed to the so-called B-band associated with a $\pi \rightarrow \pi^*$ transition,[31] together with a weak absorption at 350 nm (ε = 1870 M^{-1} cm^{-1}) due to $\pi \rightarrow \pi^*$ transitions centered on the nitro group. Upon addition of $Cu(TfO)_2$, these absorption bands shift toward shorter wavelengths as their intensity slightly decreases (Figure S1, Supporting Information). These spectral changes indicate the coordination of the pyridyl units to the metal ion. A 1:1 reaction stoichiometry was ascertained, as the data displayed a single inflection point when the Cu^{II}/H_2L molar ratio is close to one, and an isosbestic point at 290 nm. This is in agreement with the formation of mononuclear complexes. Keeping in mind the coordinating nature of DMSO, which is expected to occupy the vacant positions of the coordination sphere of the metal ions, these mononuclear complexes are denoted as $[M(H_2L)(OSMe_2)_2]^{2+}$ (M = Cu, Zn), in agreement with their optimized geometries obtained with DFT calculations. Notice that addition of an excess of Cu^{II} results in the formation of a band centered at 287 nm (ε = 3000 M^{-1} cm^{-1}) due to the formation of $[Cu(OSMe_2)_4]^{2+}$ upon addition of an excess of $Cu(TfO)_2$.[32]

Reaction of H_2L with 1 equiv of MCl_2 or hydrated $M(NO_3)_2$ or $M(SO_4)$ (M = Cu or Zn) in methanol at room temperature provided the desired complexes, which were isolated in 48−86% yields, with the noticeable exception of Cu·L·NO_3, which was obtained with a considerably lower yield (16%).

X-ray Crystal Structures. The solid state structures of Cu·L·NO_3, Cu·L·SO_4, Cu·L·Bz, and Zn·L·Cl were determined by using single crystal X-ray diffraction analyses. Bond distances

dx.doi.org/10.1021/ic402855r | Inorg. Chem. 2014, 53, 2554−2568

Table 2. Bond Distances (Å) and Angles (deg) of the Metal Coordination Environments Determined by X-ray Diffraction Measurements

	Cu·L·NO_3	Cu·L·SO_4	Cu·L·Bz	Zn·L·Cl
M(1)–N(3)		2.987(1)	2.861(3)	
M(1)–N(4)	2.038(2)	2.039(1)	2.010(3)	2.370(3)
M(1)–N(5)	1.978(2)	1.996(1)	1.961(3)	2.067(3)
M(1)–N(6)	1.93(1)	1.986(1)	1.955(3)	2.055(3)
M(1)–O(4)	2.616(9)	2.354(1)	2.637(3)	
M(1)–O(5)	1.91(1)	1.9501(9)	1.918(2)	
M(1)–O(10)	2.221(2)			
M(1)–Cl(1)				2.327(1)
M(1)–Cl(2)				2.303(1)
N(4)–M(1)–N(5)	82.88(9)	82.29(4)	84.0(1)	75.8(1)
N(4)–M(1)–N(6)		83.27(4)	84.2(1)	77.2(1)
N(4)–M(1)–O(4)		97.02(4)	84.61(9)	
N(4)–M(1)–O(5)	153.9(3)	175.25(4)	175.3(1)	
N(4)–M(1)–Cl(1)				173.41(8)
N(4)–M(1)–Cl(2)				87.97(8)
N(5)–M(1)–N(6)	158.0(3)	165.56(4)	167.2(1)	114.4(1)
N(5)–M(1)–O(4)		91.91(4)	89.8(1)	
N(5)–M(1)–O(5)	95.1(3)	96.81(4)	94.5(1)	
N(5)–M(1)–Cl(1)				98.49(9)
N(5)–M(1)–Cl(2)				129.8(1)
N(6)–M(1)–O(4)		89.68(4)	84.4(1)	
N(6)–M(1)–O(5)	98.9(4)	97.59(4)	97.7(1)	
N(6)–M(1)–Cl(1)				102.59(9)
N(6)–M(1)–Cl(2)				107.4(1)
O(4)–M(1)–O(5)		87.66(4)	99.85(9)	
Cl(1)–M(1)–Cl(2)				98.31(5)
O(10)–M(1)–N(4)	107.08(8)			
O(10)–M(1)–N(5)	93.52(7)			
O(10)–M(1)–N(6)	100.9(3)			
O(10)–M(1)–O(5)	99.0(3)			

Chart 1. Possible Conformations of $[M(H_2L)]^{2+}$ Complexes[a]

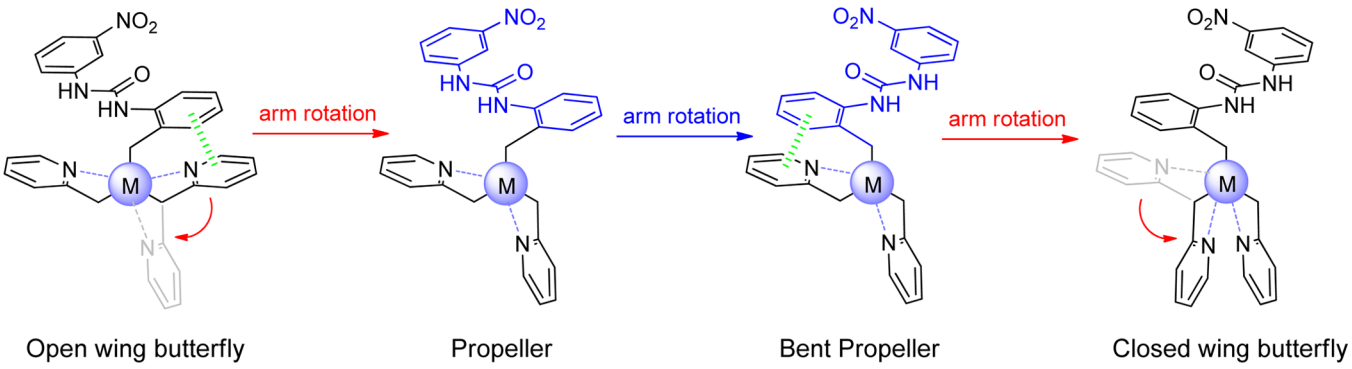

[a]Only one of the two possible enantiomers for each conformation is represented. Note that the tertiary amine nitrogen atom is placed behind the coordinated metal ion. Possible intramolecular $\pi-\pi$ stacking interactions are shown in green.

and angles of the metal coordination environments are given in Table 2.

Tridentate ligand H_2L may fold around the metal ion tilting the pyridyl and phenylurea groups with four different spatial arrangements with respect to the metal–amine axis. This gives rise to eight possible stereoisomers, existing as four enantiomeric pairs that differ in the layout of the pyridyl and phenylurea groups (Chart 1). One of these conformations resembles a propeller, with the three groups attached to the central amine atom twisting either clockwise or anticlockwise in the corresponding enantiomeric form. A second conformation would imply that the two pyridyl groups are twisted like in the "propeller" form, with the urea group bending in the opposite direction "bent propeller". The third and fourth conformations may be denoted as "open wing butterfly" and "closed wing butterfly" to emphasize the relative arrangement of the two pyridyl groups.

Crystals of Zn·L·Cl (Figure 1) contain the $[Zn(H_2L)Cl_2]$ complex and a chloroform molecule. The metal coordination environment in the $[Zn(H_2L)Cl_2]$ complex can be described as distorted trigonal bipyramidal. The equatorial plane of the trigonal bipyramid is defined by the two nitrogen atoms of the

dx.doi.org/10.1021/ic402855r | Inorg. Chem. 2014, 53, 2554–2568

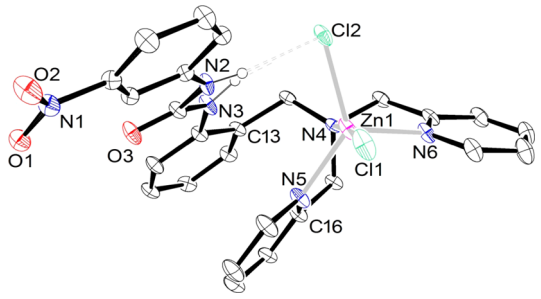

Figure 1. X-ray molecular structure of the Zn·L·Cl complex. A chloroform molecule and hydrogen atoms, except those of the urea group, are omitted for clarity. The ORTEP plot is at the 30% probability level.

pyridyl groups [N(5) and N(6)] and one of the coordinated chloride anions [Cl(2)], while the apical positions are occupied by the amine nitrogen atom of the ligand [N(4)] and the second chloride anion [Cl(1)]. The metal ion is placed 0.36 Å above the plane defined by the three donor atoms of the equatorial plane. The N−M−N and Cl−M−N angles of the equatorial plane (107−130°) are relatively close to those expected for a regular trigonal bipyramidal coordination, while the N(4)−M−Cl(1) angle (*ca.* 173.4°) deviates by less than 7° from the ideal one (180°). This is in line with the value of the index of trigonality τ, which amounts to 0.73 (τ = 0 for a perfect square-pyramidal geometry and τ = 1 for an ideal trigonal bipyramidal geometry).[33] The Zn(1)−N(5) and Zn(1)−N(6) distances are similar to those observed for different five-coordinated Zn^{II} complexes with tripodal ligands containing pyridyl units (2.02−2.09 Å), while the Zn(1)−N(4) distance (2.370 Å) is somewhat longer than those observed for related complexes with tripodal ligands.[34]

The 'bent propeller' conformation adopted by the ligand in the $[Zn(H_2L)Cl_2]$ complex is imposed by the presence of intramolecular slipped $\pi-\pi$ stacking interactions involving the pyridyl ring containing N(5) and the benzylurea fragment.[35] The 1-(3-nitrophenyl)-3-benzylurea fragment is nearly planar, with mean deviation from planarity of 0.06 Å. The mean-square planes defined by the 1-(3-nitrophenyl)-3-benzylurea and pyridyl fragments intersect at 18.1°, and the shortest contacts between them correspond to the N3···N5 (3.193 Å) and C13···C16 (2.964 Å) distances. This conformation appears to favor $N_{pyridyl}$-M-$N_{pyridyl}$ angles of about 120°, and therefore a trigonal bipyramidal coordination environment.

The coordinated chloride anion Cl(2) is involved in a bifurcated hydrogen-bonding interaction with the NH groups of the urea fragment (Table 3).[36] The N(2)···Cl(2) distance is somewhat shorter than the N(3)···Cl(2) one, while the N(2)−H(2)···Cl(2) angle is closer to linearity in comparison with the N(3)−H(3)···Cl(2) one. This indicates a stronger interaction of the chloride anion with N(2). The D-H···Cl interactions were categorized in three groups depending on the observed H···Cl distances: short (≤2.52 Å), intermediate (2.52−2.95 Å), and long (2.95−3.15 Å).[37] The N−H···Cl contacts observed can be therefore regarded as intermediate [N(3)−H(3)···Cl(2)] or short [N(2)−H(2)···Cl(2)]. It was suggested that hydrogen bonds involving N−H donors and Cl−M acceptors (M = transition metal) are favored for M−Cl···H angles in the range 100−110°.[38] The values observed for the Zn^{II} complex reported here (~80°, Table 3) are somewhat smaller, but they point to an angular preference for angles close to the perpendicular approach probably because of the higher basicity of the halogen p-type lone pairs relative to the sp lone pair.[38]

The crystal packing is determined by intermolecular halogen-bonding interactions between the oxygen atoms of the nitro group and a chloroform molecule that is bridging two complex units, assisted by weak C−H···Cl hydrogen bonds with the coordinated chloride anions. The two C−Cl···O distances [Cl(3)···O(2) 3.12 Å, C−Cl(3)···O(2) 161.47° and Cl(5)···O(1) 3.09 Å, C−Cl(5)···O(1) 147.37°] are shorter than the sum of the van der Waals radii of Cl and O (1.75 and 1.52 Å, respectively).[39] However, the C−Cl···O angles deviate considerably from the ideal value of 180°, which points to rather weak interactions.

Crystals of $Cu{\cdot}L{\cdot}NO_3$ contain the $[Cu(H_2L)(ONO_2)(OHMe)]^+$ cation and a nitrate anion interacting with the urea group of the ligand through a bifurcated hydrogen bond (Figure 2). The ligand wraps around the metal ion, giving an

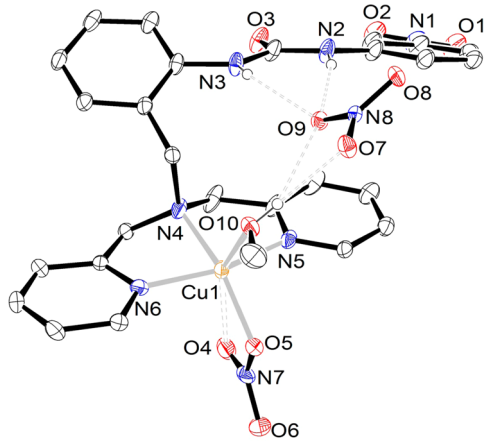

Figure 2. X-ray molecular structure of $Cu{\cdot}L{\cdot}NO_3$. Hydrogen atoms, except those involved in hydrogen-bonding interactions, are omitted for clarity. The ORTEP plot is at the 30% probability level.

"open wing butterfly" conformation. The 3-nitrophenyl group and the N(2)−C(7)−O(3) fragment of the urea group are nearly coplanar, with the corresponding least-squares plane (mean deviation from planarity 0.045 Å) intersecting with the least-squares plane defined by the benzyl group and N(3) at 47.5°. This value clearly shows that the 1-(3-nitrophenyl)-3-benzylurea unit is not planar, in contrast to the situation observed for the $[Zn(H_2L)Cl_2]$ complex. Most likely this is to

Table 3. Intramolecular Hydrogen Bonds Involving the Urea Group in Zn·L·Cl

	d(D−H)	*d*(H···A)	*d*(D···A)	∠(DHA)	∠(ZnClH)
N(2)−H(2)···Cl(2) Å/deg	0.85	2.42	3.240(3)	163.6	
N(3)−H(3)···Cl(2) Å/deg	0.85	2.58	3.352(3)	152.2	
Zn−Cl(2)···H(2)/deg					80.9
Zn−Cl(2)···H(3)/deg					78.7

dx.doi.org/10.1021/ic402855r | *Inorg. Chem.* 2014, 53, 2554−2568

Table 4. Hydrogen Bonds in Compounds Involving the Urea Group in Cu^{II} Complexes

	d(D−H)	d(H···A)	d(D···A)	∠(DHA)	∠(XOH)
		Cu·L·SO_4			
N(2)−H(2)···O(6) Å/deg	0.78(2)	2.06(2)	2.834(1)	169.2(2)	
N(3)−H(3)···O(8) Å/deg	0.80(2)	2.03(2)	2.819(1)	169.8(2)	
S(1)−O(6)···H(2)/deg					112.3
S(1)−O(8)···H(3)/deg					107.2
		Cu·L·NO_3			
N(2)−H(2)···O(9) Å/deg	0.80(3)	2.10(3)	2.857(3)	160(3)	
N(3)−H(3)···O(9) Å/deg	0.75(3)	2.26(3)	2.928(3)	149(3)	
N(8)−O(9)···H(2)/deg					116.3
N(8)−O(9)···H(3)/deg					140.3
		Cu·L·Bz			
N(2)−H(2)···O(7) Å/deg	0.79	2.21	2.976(3)	161.5	
N(3)−H(3)···O(8) Å/deg	0.75	2.12	2.771(3)	145.5	
C(34)−O(7)···H(2)/deg					99.3
C(34)−O(8)···H(3)/deg					126.4

maximize the hydrogen-bonding interaction of the non-coordinated nitrate anion with the urea group of the ligand.

Ligand H_2L binds to the Cu^{II} ion in a distorted octahedral coordination where the equatorial plane of the octahedron is defined by the three nitrogen atoms of the dpa unit [N(4), N(5), and N(6)] and an oxygen atom of a coordinated nitrate anion [O(5)]. The apical positions are occupied by the oxygen atom of a methanol molecule [O(10)] and one of the oxygen atoms of the nitrate anion [O(4)], both placed along the ideal C_4 perpendicular axis. The Cu(1)−O(10) and Cu(1)−O(4) distances are very long, as expected for a tetragonal elongation due to a strong Jahn−Teller distortion.[40] The mean deviation from planarity of the donor atoms of the equatorial plane is 0.11 Å, with the Cu^{II} ion being placed 0.335 Å above that plane. The Cu(1)−O(10) distance [2.221(2) Å] is *ca.* 0.2−0.3 Å longer than the distances to the donor atoms of the equatorial plane. The *cis* angles of that plane range between 77.1 and 98.9° and, therefore, are reasonably close to the expected values of a regular geometry (90°). The angles defined by the Cu(1)−O(10) vector and the donor atoms of the equatorial plane (93.5−107.1°) are also relatively close to the expected value (90°).

The geometrical data characterizing the asymmetrical bifurcated hydrogen bond involving the urea group and the uncoordinated nitrate anion are shown in Table 4. Both the N···O(9) distances and N−H···O(9) angles point to a stronger interaction of the anion with the hydrogen-bonding donor N(2) compared with N(3). The N(8)−O(9)···H(2) angle (116.3°) is close to the ideal value of 115 ± 10°,[41] while the larger value of the angle N(8)−O(9)···H(3) (140.3°) also reflects a weaker interaction. Furthermore, the dihedral angles O(8)−N(8)−O(9)-H(2) and O(7)−N(8)−O(9)-H(2) (4.2 and 174.7°, respectively) are close to the values providing strong interactions (0° and 180°), while the corresponding values involving H(3) deviate considerably from the ideal angles [O(8)−N(8)−O(9)−H(3) = 71.1° and O(7)−N(8)−O(9)−H(3) = 107.7°]. The interaction of the nitrate anion with the urea receptor appears to also be reinforced by weak C−H···O interactions involving oxygen atoms of the nitrate anion and C−H groups of the 1-(3-nitrophenyl)-3-benzylurea unit. Finally, a strong hydrogen-bonding interaction also exists between the O−H group of the coordinated methanol molecule and one of the oxygen atoms of the nitrate anion [O(10)···O(7) 2.740(2) Å; O(10)−H(10)···O(7) 2.00(4) Å; O(10)−H(10)−O(7) 161(4)°].

Crystals of Cu·L·SO_4 (Figure 3) contain the [Cu(H_2L)(OH_2)(OS(O)$_2$O)] complex and two water molecules of crystallization that form a hydrogen-bonding network with O(7) and O(8), while those of Cu·L·Bz contain the [Cu(H_2L)(O_2CPh)(OH_2)]···O_2CPh entity (O_2CPh = Bz^-). Again, the Cu^{II} ions also present a distorted octahedral coordination with a strong Jahn−Teller distortion.[40] The equatorial plane of the octahedron is defined by the three

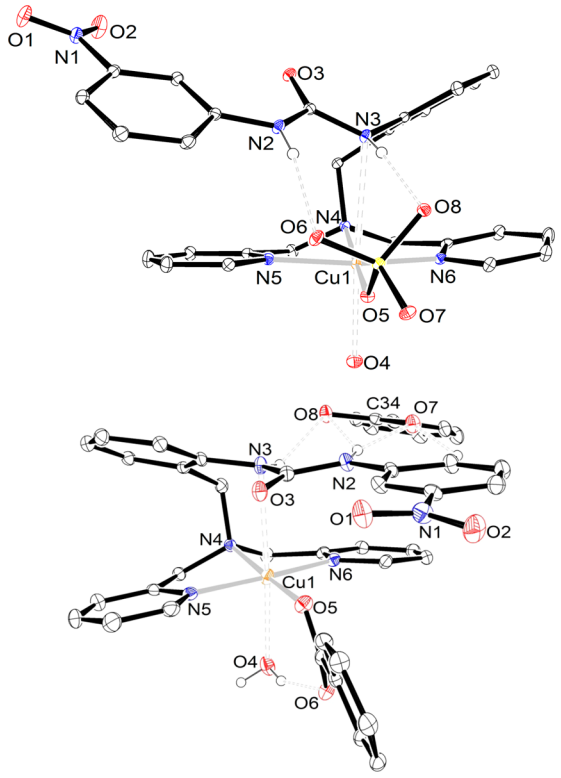

Figure 3. X-ray molecular structures of Cu·L·SO_4 (top) and Cu·L·Bz (bottom). Hydrogen atoms, except those involved in hydrogen-bonding interactions, are omitted for clarity. Two water molecules present in the crystal lattice of Cu·L·SO_4 are also omitted. The ORTEP plots are at the 30% probability level.

dx.doi.org/10.1021/ic402855r | *Inorg. Chem.* 2014, 53, 2554−2568

nitrogen atoms of the dpa unit [N(4), N(5), and N(6)] and an oxygen atom of a coordinated sulfate or benzoate anion [O(5)], while the apical positions are occupied by one of the nitrogen atoms of the urea group [N(3)] and the oxygen atom of the water molecule [O(4)] placed along the ideal C_4 perpendicular axis. The *cis* angles among the donor atoms of the equatorial plane range between 82.3 and 97.7°, while the corresponding *trans* angles fall in the range 165.6−175.3°, pointing to relatively small distortions of the metal coordination environments. Both complexes show an "open wing butterfly" conformation, but the conformation of the 1-(3-nitrophenyl)-3-benzylurea unit changes considerably depending on the particular anion. Indeed, the least-squares plane defined by the 3-nitrophenyl group and the N(2)−C(7)−O(3) fragment forms an angle of 55.8° with the plane defined by the benzyl group and N(3) in the sulfate complex, while this angle is much smaller (47.5°) in the case of the nitrate anion. These very different values are probably related to the different shapes of the two anions. In the case of the sulfate complex, cooperative binding involving simultaneous anion coordination to the urea H-donor group and Cu^{II} is observed. However, in the benzoate analogue the urea moiety and the metal ion interact each with a different benzoate anion. The coordinated water molecule in $[Cu(H_2L)(O_2CPh)(OH_2)]\cdots O_2CPh$ shows hydrogen-bonding with an oxygen atom of the coordinated benzoate anion [O(4)···O(6) 2.709(3) Å; O(4)−H(2W)···O(6) 1.89(4) Å; O(4)−H(2W)−O(6) 159(4)°].

Both sulfate and benzoate anions provide a Y-shape directional hydrogen-bonding interaction with the urea fragment. The geometrical data characterizing the H-bonds (Table 4) point to a rather symmetrical interaction of the sulfate anion with the urea receptor, with the two N−H···O contacts showing very similar distances and angles. In the case of the benzoate analogue, this interaction is less symmetrical, and the N(urea)−O(benzoate) distances observed (2.770 and 2.975 Å) situate them within the group of "moderate" hydrogen bonds according to Jeffrey's classification.[42] Furthermore, while the C(34)−O(7)···H(2) and C(34)−O(8)···H(3) angles are relatively close to the ideal value for a trigonal planar anion (115 ± 12°),[41] the O(8)−C(34)−O(7)−H(2) and O(7)−C(34)−O(8)−H(3) dihedrals (18.7 and 45.8°, respectively) deviate considerably from the ideal values (0 and 180°). In the case of the sulfate anion, both the S(1)−O(6)−H(2) and S(1)−O(8)−H(3) angles are close to the ideal value (122 ± 12°).[43] Taken together, the data given in Table 4 indicate a stronger interaction of the sulfate anion with the urea unit compared with nitrate and benzoate anions.

Solution Structure. Before studying the ability of the Cu^{II}-based ditopic receptor for anion recognition, we investigated the structure of the Zn^{II} analogue in solution in the presence of different coordinating anions by using NMR spectroscopy. The experiments were carried out in DMSO-d_6 due to the low solubility of these systems in water. Addition of 1 equiv of $MeCO_2^-$, HSO_4^-, or $H_2PO_4^-$ (as their tetrabutylammonium salts) to a solution of the free receptor causes important shifts of the two N−H signals that reflect the establishment of directional H-bond interactions with these oxoanions. In the case of $MeCO_2^-$, both proton signals experience a downfield shift to 11.93 and 11.16 ppm, respectively (Figure 4). A similar spectral pattern is also observed for $H_2PO_4^-$ (11.16 and 10.52 ppm) whereas addition of HSO_4^- provokes negligible chemical shift changes (10.32 and 9.57 ppm), pointing to a rather weak interaction. On the contrary, addition of a spherical anion such

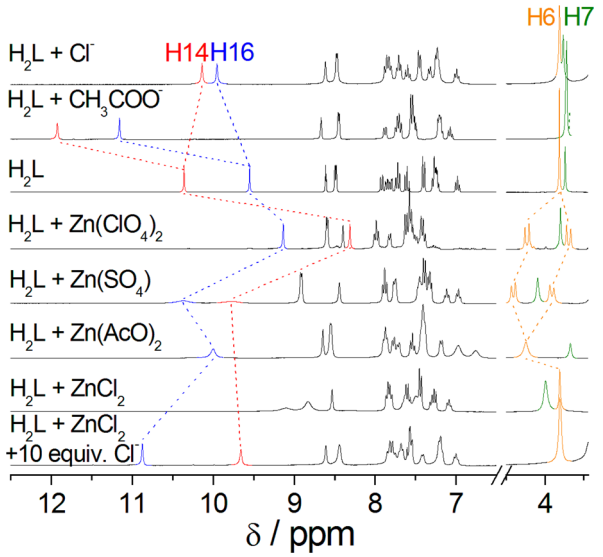

Figure 4. ^{1}H NMR spectrum (300 MHz, DMSO-d_6) of H_2L and spectra recorded after addition of $[Bu_4N]\cdot Cl$, $[Bu_4N]\cdot MeCO_2$, or different Zn^{II} salts [H_2L/Zn^{II} (1:1) ensemble (40 mM)].

as Cl^- causes the deshielding of H16 (9.95 ppm) and a concomitant shielding of H14 (10.14 ppm), which indicates an asymmetrical H-bond interaction where only H16 is interacting with the anion. Anion binding polarizes the N−H16 bond, and therefore, the ^{1}H NMR signal of this proton is deshielded (through-space effect). The increased partial negative charge on the nitrogen atom of the N−H14 group is then delocalized over the urea moiety (through-bond effect), thereby inducing the shielding of H14.[14b,16d,44]

The presence of Zn^{II} in solution drives to a different situation. Upon coordination of the metal ion, the signals of the protons corresponding to the aromatic region shift with respect to their positions in the free ligand and overlap as complicated multiplets, which prevented their unequivocal assignment. However, the proton signals of the NH urea fragment and those of protons H6 and H7 can still be used to monitor the interaction of the anion with the metal-based receptor. Thus, addition of $Zn(ClO_4)_2$ provokes an important shielding of the N−H resonances, in particular that corresponding to H14, which experiences an upfield shift of *ca.* 2 ppm from 10.30 to 8.31 ppm while the signal due to H16 shifts upfield by 0.44 ppm from 9.58 to 9.14 ppm. These unprecedented upfield shifts of the signals due to urea N−H protons can only be explained by the coordination of the urea group to the Zn^{II} ion. Indeed, the signal due to protons H6, which is observed as a singlet in the ^{1}H NMR spectrum of the free ligand, is now observed as an AB spin system (^2J = 16 Hz) upon addition of $Zn(ClO_4)_2$. It has been shown that Zn^{II} complexes with symmetrical tripodal ligands with "propeller-like" structures provide single-line spectra due to a fast enantiomerization process that does not require the cleavage of the Zn-donor bonds.[45] Thus, the diastereotopic nature of the signals due to H6 is most likely an indication of an "open wing butterfly' structure. Zn^{II} complexes prepared with other weakly coordinating anions such as TfO^- provide identical spectra, indicating a similar behavior of the metal-based receptor with this anion. We notice that the molar conductivity value obtained for this complex in methanol (184 $cm^2\ \Omega^{-1}\ mol^{-1}$) is in agreement with a 2:1 electrolyte behavior, which indicates

dx.doi.org/10.1021/ic402855r | Inorg. Chem. 2014, 53, 2554−2568

that the perchlorate anion does not interact with the cation complex in solution.

The ^{1}H NMR spectrum of $[Zn(H_2L)(SO_4)]$ (Figure 4) shows that sulfate binding provokes an important deshielding and broadening of the urea NH proton signals, which are observed at 9.76 and 10.36 ppm. These chemical shift changes are attributed to the formation of H-bonds between the anion and the NH groups of the urea moiety, with concomitant decoordination of the nitrogen atom of the urea unit upon anion addition. On the other hand, the presence of 2 equiv of a more basic anion such as acetate causes the deprotonation of the urea unit, as the N−H14 signal disappears, while the resonance due to N−H16 experiences a slight deshielding. The addition of D_2O to a solution of the Zn^{2+} complex in the presence of 2 equiv of acetate causes the attenuation of the N−H16 signal, while the 9.0−6.5 region remains unaffected, which supports the deprotonation process (Figure S8, Supporting Information). We also notice that the signals due to H6 protons become a singlet upon $MeCO_2^-$ addition, which is indicative of a "propeller-like" structure of the complex in solution. A similar conformation is probably adopted in the presence of 2 equiv of Cl^-, where the H6 protons are also shown as a singlet. However, in this case the signals due to the NH urea protons are quite broad, reflecting dynamic exchange processes, with their unequivocal assignment being impossible. This broadening may be related to the presence of a dynamic exchange process between a 1:1 electrolyte and a nonelectrolyte species in solution, as suggested by the conductivity value obtained for this complex in methanol (68 $cm^2\ \Omega^{-1}\ mol^{-1}$). Nonetheless, in the ^{1}H NMR spectrum of the Zn^{II} complex recorded in the presence of 10 equiv of Cl^-, the urea NH proton signals appear at 10.88 (H16) and 9.66 ppm (H14). These shifts indicate an important deshielding of the NH signals upon Cl^- addition, which is in line with the decoordination of the urea group and the establishment of a hydrogen-bonding interaction between urea and the coordinated Cl^- anions. This situation has also been observed in the crystal molecular structure of Zn·L·Cl described above.

As seen in the molecular crystal structures of Cu·L·SO_4 and Cu·L·Bz (*vide supra*), a weak interaction between the nitrogen atom of the urea group N(3) and the Cu^{II} ion is observed. The metal coordination environment in Cu^{II} complexes appears to be conditioned by a strong Jahn−Teller distortion that results in very long Cu(1)−N(3) and Cu(1)−O(4) distances. One could expect that these distances were shorter in the complexes of the d^{10} metal ion Zn^{II}. Unfortunately, we have not obtained single crystals of the Zn(II) perchlorate complex, but the minimized geometries obtained by DFT calculations (TPSSh/SVP) on the $[M(H_2L)(OSMe_2)_2]^{2+}$ systems (M = Cu, Zn) in DMSO solution are in agreement with this hypothesis. The optimized geometry of $[Cu(H_2L)(OSMe_2)_2]^{2+}$ presents Cu(1)−N(3) and Cu(1)−O(4) distances of 2.680 Å and 2.228 Å, respectively, while the remaining four donor atoms of the ligand provide considerably shorter Cu-donor bonds (2.03−2.08 Å, Figure 5). This is in line with an octahedral coordination around Cu^{II} with strong Jahn−Teller distortion. Analogous calculations performed on the $[Zn(H_2L)(OSMe_2)_2]^{2+}$ complex indicate octahedral coordination around the metal ion with a Zn(1)−N(3) distance of 2.621 Å. Although longer than the remaining bond distances of the metal coordination environment, which fall within the range 2.08−2.29 Å, these data clearly indicate a weak coordination of the nitrogen atom of the urea group N(3) to the metal ion

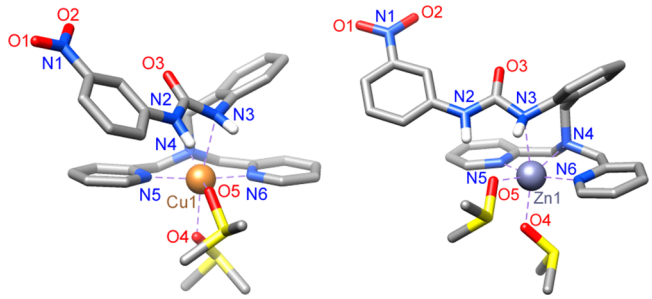

Figure 5. Geometries of the $[M(H_2L)(OSMe_2)_2]^{2+}$ complexes (M = Cu or Zn) obtained from DFT calculations (TPSSh/SVP level) in DMSO solution. Cu(1)−N(3) 2.680 Å, Cu(1)−N(4) 2.080 Å, Cu(1)−N(5) 2.041 Å, Cu(1)−N(6) 2.037 Å, Cu(1)−O(4) 2.228 Å, Cu(1)−O(5) 2.029 Å, Zn(1)−N(3) 2.621 Å, Zn(1)−N(4) 2.289 Å, Zn(1)−N(5) 2.107 Å, Zn(1)−N(6) 2.118 Å, Zn(1)−O(4) 2.079 Å, Zn(1)−O(5) 2.096 Å.

(Figure 5), as suggested by the shift of H(14) in the ^{1}H NMR spectrum in the presence of $Zn(ClO_4)_2$ (*vide supra*). Further support for the coordination of this urea nitrogen atom comes from the ^{13}C NMR spectra, where the signal due to the carbon nucleus of the urea group is observed at 152.6 ppm for H_2L but experiences a deshielding to 153.3 ppm in the perchlorate salt of the Zn^{II} complex. Complexation of substituted ureas to Cu^{II} or Zn^{II} is very rare, and to the best of our knowledge there is only one example of a Cu^{II} complex where an aromatic urea group coordinates via the nitrogen atom.[46]

DFT calculations performed on the $[Zn(H_2L)(OSMe_2)(OS(O)_2OH)]^+$ complex give a Zn(1)−N(3) distance of 2.441 Å (Figure 6), which represents a slight shortening of *ca.* 0.18 Å

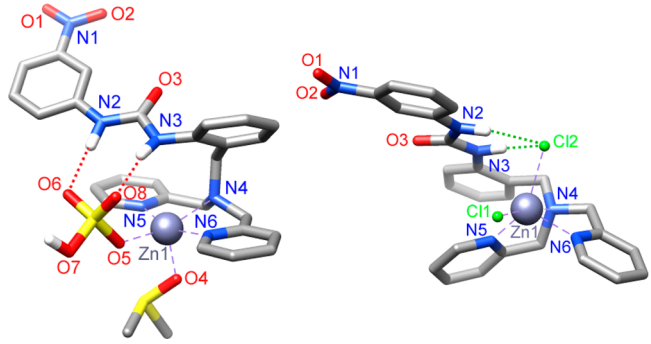

Figure 6. Geometries of the $[Zn(H_2L)(OS(O)_2OH)(OSMe_2)]^+$ (left) and $[Zn(H_2L)Cl_2]$ (right) complexes obtained from DFT calculations (TPSSh/SVP level) in DMSO solution. Hydrogen atoms, except those involved in hydrogen-bonding interactions, are omitted for the sake of simplicity.

with respect to the distance obtained for $[Zn(H_2L)(OSMe_2)_2]^{2+}$ (Figure 5). The anion binds to the urea group through directional H-bonds, in line with the deshielding of the ^{1}H NMR signals of the NH groups observed upon sulfate addition. Furthermore, the AB spin system (^2J = 16 Hz) observed for protons H6 pointed to an "open wing butterfly" structure of this complex in solution, in agreement with the DFT optimized geometry obtained for HSO_4^- adduct. A similar structure was observed for the Cu^{II} analogue in the X-ray molecular structure of Cu·L·SO_4 described above. Taken together, these results indicate that tetrahedral anions such as HSO_4^- and SO_4^- are recognized in solution through a cooperative binding involving H-bonding interaction with the

dx.doi.org/10.1021/ic402855r | *Inorg. Chem.* 2014, 53, 2554−2568

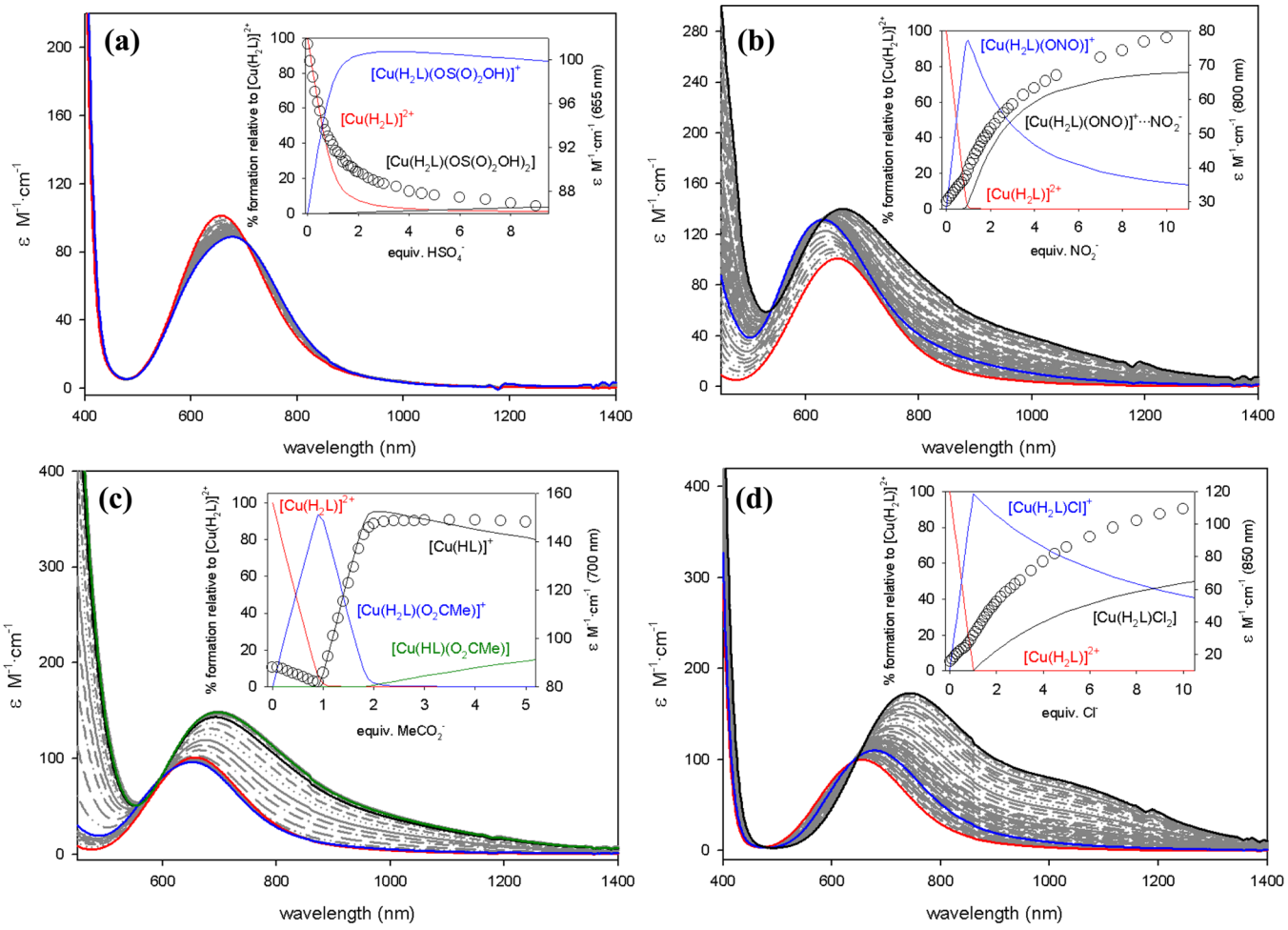

Figure 7. Family of UV/vis spectra taken during the course of the titration of $[Cu(H_2L)(OSMe_2)_2]^{2+}$ (5×10^{-3} M in DMSO) with a standard solution (0.5 M in DMSO, 25 °C): (a) $[Bu_4N]\cdot HSO_4$; (b) $[Bu_4N]\cdot NO_2$; (c) $[Bu_4N]\cdot MeCO_2$; and (d) $[Bu_4N]\cdot Cl$. Inset: titration profile at a selected wavelength vs equivalents of anion and species distribution diagram (coordinated DMSO molecules were omitted for the sake of simplicity).

urea unit of the ligand and coordination to the metal ion (Cu^{II} or Zn^{II}).

The optimized geometry obtained for the $[Zn(H_2L)Cl_2]$ complex in solution (Figure 6) shows a cooperative binding on anion recognition where the nitrogen atom of the urea fragment N(3) is not coordinated to the metal ion. This situation has been observed in the X-ray molecular structure of Zn·L·Cl and is also in line with the shifts of the NH proton signals of the urea group seen in the ^{1}H NMR spectra. DFT calculations provide a very similar structure for the Cu^{II} analogue.

Study of the Interaction with Oxoanions. The interaction of $[Cu(H_2L)(OSMe_2)_2]^{2+}$ (prepared *in situ* by mixing stoichiometric amounts of H_2L and $Cu(TfO)_2$) with different oxoanions such as NO_3^-, NO_2^-, HSO_4^-, $H_2PO_4^-$, $MeCO_2^-$, and $PhCO_2^-$ was followed by spectrophotometric titrations in DMSO solution. For comparative purposes, we have also investigated the interaction of the free ligand with the corresponding tetrabutylammonium salts of these anions. The results show that only acetate establishes weak H-bond interactions with the free ligand (Figure S2, Supporting Information). The titration profile and the presence of only one isosbestic point at 360 nm indicates the presence of a single equilibrium in solution, in agreement with the formation of a 1:1 ($MeCO_2^-/H_2L$) adduct. The smooth curvature of the titration profile is characteristic of a very weak binding, which prevents an accurate calculation of the association constant.

Solutions of the Cu^{II} complex (5×10^{-3} M) were titrated with standard solutions of the different oxoanions (as their tetrabutylammonium salts) up to a 10-fold excess. The absorption spectrum of $[Cu(H_2L)(OSMe_2)_2]^{2+}$ shows a broad band in the range 500−1200 nm with a maximum at 656 nm (ε = 100 M^{-1} cm^{-1}) characteristic of *d*−*d* transitions centered on the Cu^{II} metal ion. These spectral data are very similar to those reported for the Jahn−Teller distorted octahedral perchlorate derivative $[Cu(dpa)(OHMe)](ClO_4)_2$ (dpa = di(2-picolyl)amine) and related complexes,[47] which match the predictions of our DFT calculations. Thus, this band is attributed to the $d_{xz},d_{yz} \rightarrow d_{x^2-y^2}$ ($^2B_1 \rightarrow {}^2E$) transition in a tetragonal ligand field.[48] The molar conductivity value obtained for the perchlorate analogue in methanol (164 cm^2 Ω^{-1} mol^{-1}) is in agreement with a 2:1 electrolyte behavior, confirming that weakly coordinating anions such as ClO_4^- or TfO^- do not interact with the cation complex in solution.

Addition of NO_3^- up to a 20-fold excess only provokes slight changes in the absorption spectra, indicating a very weak binding of this anion to the metal complex. Indeed, the intermediate value obtained for the conductivity of this complex in methanol (137 $cm^2\Omega^{-1}$ mol^{-1}) is indicative of the presence of an equilibrium in solution between 2:1 and 1:1

dx.doi.org/10.1021/ic402855r | Inorg. Chem. 2014, 53, 2554−2568

Table 5. Spectroscopic Data and Association Constants (log K Values) Obtained from Spectrophotometric Titrations in DMSO Solutions (25 °C)

	$[Cu(H_2L)(X)]^+$		$[Cu(H_2L)(X)_2]$	
X	log K_{11}	λ_{max}, nm (ε, $M^{-1}\cdot cm^{-1}$)	log K_{12}	λ_{max}, nm (ε, $M^{-1}\cdot cm^{-1}$)
$MeCO_2^-$	>7	653 (96)		
Cl^-	>7	678 (109)	1.48(1)	744 (173)
NO_2^-	5.46(9)	629 (109)	2.11(1)	664 (140)
$H_2PO_4^-$	3.81(4)	684 (86)	2.29(1)	720 (83)
Br^-	3.81(6)	679 (141)	1.14(1)	737 (197)
HSO_4^-	3.37(9)	679 (89)		

electrolyte species. However, addition of HSO_4^- to a solution of $[Cu(H_2L)(OSMe_2)_2]^{2+}$ causes a red shift of the d–d band as its intensity decreases, pointing to the coordination of the anion to the metal center (Figure 7a), which retains a distorted octahedral geometry. The titration profile and the formation during the course of the titration of two simultaneous isosbestic points at 540 and 705 nm are indicative of the presence of a single equilibrium in solution, which is in agreement with the formation of a 1:1 complex. The analysis of the titration data provided an association constant of log K_{11} = 3.37(9) (Table 5).

In contrast to the situation observed for HSO_4^-, two different processes could be identified during the course of the titration of Cu^{II} complex with NO_2^- (Figure 7b). Addition of up to 1 equiv of NO_2^- results in the coordination of the anion to the metal ion to form a 1:1 ($[Cu(H_2L)]^{2+}/NO_2^-$) complex (eq 1). Addition of a second equivalent of NO_2^- provokes a drastic structural change evidenced by the important variations observed in the absorption spectra (eq 2) (solvent molecules were omitted for the sake of clarity):

$$[Cu(H_2L)(OSMe_2)_2]^{2+} + X^- \leftrightarrows [Cu(H_2L)(X)(OSMe_2)]^+ + OSMe_2 \quad (1)$$

$$[Cu(H_2L)(X)(OSMe_2)]^+ + X^- \leftrightarrows [Cu(H_2L)(X)(OSMe_2)]^+\cdots X^- \quad (2)$$

$$[Cu(H_2L)(X)(OSMe_2)]^+ + X^- \leftrightarrows [Cu(H_2L)(X)_2] + OSMe_2 \quad (3)$$

The spectral changes recorded upon addition of $H_2PO_4^-$ to a solution of $[Cu(H_2L)(OSMe_2)_2]^{2+}$ in DMSO are very similar to those observed for NO_2^- (Figure S3, Supporting Information), indicating that both anions provide a very similar behavior described by eqs 1 and 2. The equilibrium constants determined for these processes amount to log K_{11} = 5.46(9) and log K_{12} = 2.11(1) for NO_2^- and log K_{11} = 3.81(4) and log K_{12} = 2.29(1) for $H_2PO_4^-$, respectively.

In the case of NO_2^- anion, the spectral changes for the second step indicate the formation of a complex species with trigonal bipyramidal coordination around the Cu^{II} ion. Indeed, trigonal bipyramidal Cu^{II} complexes usually exhibit a broad band extending from 500 to 1000 nm with two components.[49] Although the low energy band is often more intense than the high-energy counterpart, in the present case this situation appears to be reversed, with the band envelope showing a shoulder on the low energy side. In this case, the three nitrogen atoms of the dpa unit and one nitrogen atom of the urea group also bind to the metal center as seen for Cu·L·Bz. The coordination polyhedron might be completed with a monodentate nitrite anion giving the expected trigonal bipyramidal geometry, with the second nitrite anion being involved in a hydrogen-bonding interaction with the N-coordinated urea group.

Addition of acetate to a solution of $[Cu(H_2L)(OSMe_2)_2]^{2+}$ gives rise to a more intricate behavior with very important changes in the d–d absorption band (Figure 7c). The intensity of the band at 656 nm decreases while experiencing a slight blue shift to 653 nm, reaching the lowest absorption after addition of 1 equiv of anion. After that, the intensity of the d–d transition band suddenly increases as its maximum shifts to 699 nm. At the same time, the tail of a ligand-centered charge transfer band from the −NH fragment to the $-NO_2$ group, characteristic of the deprotonation of the receptor, is also observed in the high energy side of the spectrum. This CT band is clearly observed when the titration is performed at low concentration (10^{-4} M) (see also Figure S6, Supporting Information).[14b,c] The titration profile shows a second inflection point at a 1:2 ($[Cu(H_2L)]^{2+}/MeCO_2^-$) stoichiometry. Further addition of an excess of anion results in subtle changes in the absorption spectrum.

These data are rationalized in terms of the formation of three different species in solution upon acetate addition. The first species formed during the course of the titration is characterized by a very high association constant (log K > 7.0) and is attributed to the coordination of the anion to the metal center according to the following:

$$[Cu(H_2L)(OSMe_2)_2]^{2+} + MeCO_2^- \leftrightarrows [Cu(H_2L)(O_2CMe)(OSMe_2)]^+ + OSMe_2 \quad (4)$$

The second process represents deprotonation of the urea moiety according to equilibrium 5, which involves the formation of a hydrogen-bond complex between acetate and its conjugated acid:[14c]

$$[Cu(H_2L)(O_2CMe)(OSMe_2)]^+ + MeCO_2^- \leftrightarrows [Cu(HL)(OSMe_2)]^+ + [(MeCO_2)_2H]^- \quad (5)$$

The analysis of the titration data provides a pK_a value of 10.12(3). This value is 17 orders of magnitude lower than that of urea (pK_a = 26.9 in DMSO)[50] and ∼9 units lower than the value reported for N,N'-diphenylurea (pK_a = 18.7 in DMSO).[51] The urea group in $[Cu(H_2L)(O_2CMe)]^+$ is even considerably more acidic than that of 1-(3,5-bis(trifluoromethyl)phenyl)-3-phenylurea (pK_a = 16.1 in DMSO),[51] which contains two $-CF_3$ substituents with strong electron-withdrawing ability. Thus, the deprotonation of the urea moiety in $[Cu(H_2L)(O_2CMe)]^+$ can only be explained by its N-coordination to the metal ion. The deprotonation of the Zn^{II} analogue after addition of 2 equiv of acetate has also been observed in the ^1H NMR spectrum where

dx.doi.org/10.1021/ic402855r | Inorg. Chem. 2014, 53, 2554−2568

one of the NH signals of the urea group disappears, while the second NH signal experiences a slight deshielding (*vide supra*). The red shift observed in the *d*−*d* transitions of the Cu^{II} complex is also indicative of a structural change from the Jahn−Teller distorted octahedral coordination to a trigonal bipyramidal geometry upon complex deprotonation (see above). Addition of an excess of $MeCO_2^-$ results in the formation of an additional species, presumably due to the coordination of the anion to the metal ion according to the following:

$$[Cu(HL)(OSMe_2)]^+ + MeCO_2^- \leftrightarrows [Cu(HL)(O_2CMe)] + OSMe_2 \quad (6)$$

The equilibrium constant determined for this process is low and amounts to log K = 1.06(3).

Addition of $PhCO_2^-$ to a solution of $[Cu(H_2L)]^{2+}$ in DMSO provokes spectral changes very similar to those observed upon $MeCO_2^-$ addition (Figure S4, Supporting Information), indicating that reactions 3−5 are also valid to account for the speciation in solution in the presence of $PhCO_2^-$. The pK_a value of the urea group obtained from the titration with $PhCO_2^-$ (pK_a = 9.30) is very similar to that obtained for $MeCO_2^-$, while the association constant for the third step [log K = 1.09(3), eq 6] is identical within experimental error.

Study of the Interaction with Halides. In the absence of a bound metal ion, halide anions (except F^-) establish very weak H-bond interactions with the ligand, which prevented the determination of reliable association constants for the formation of 1:1 adducts. As previously observed for the oxoanions, the intramolecular hydrogen-bonding interactions between the NH fragment of the urea moiety and the pivotal nitrogen of the dpa unit block the anion binding site, which results in the observed weak interaction with Cl^- (Figure 4).

Addition of Cl^- or Br^- to a solution of $[Cu(H_2L)(OSMe_2)_2]^{2+}$ in DMSO provokes a slight red shift of the *d*−*d* absorption band from 656 to 678 nm (Cl^-) and 679 nm (Br^-) up to 1 equiv of added halide anion (Figure 7d; see also Figure S5, Supporting Information). Addition of an excess of anion results in the formation of a very broad *d*−*d* absorption band with a maximum at 744 nm (Cl^-) and 737 nm (Br^-), characteristic of a trigonal bipyramidal coordination around the metal ion.

The spectral changes can be rationalized in terms of the equilibria (eqs 1 and 3) where the first step involves the coordination of an X^- anion to the metal ion by replacing a coordinated DMSO molecule. The resulting $[Cu(H_2L)(OSMe_2)(X)]^+$ cation retains the Jahn−Teller distorted tetragonal geometry of the $[Cu(H_2L)(OSMe_2)_2]^{2+}$ species, as indicated by the corresponding absorption profiles. The second step implies the coordination of a second X^- anion to the metal ion with a concomitant change of the metal coordination environment to trigonal bipyramidal $[Cu(H_2L)(X)_2]$, where the Cu^{II} complex presents a "bent propeller" conformation with cooperative binding mode observed in the X-ray molecular structure of $[Zn(H_2L)Cl_2]$ (Figure 1). The structural analysis performed by ^1H NMR spectroscopy for the related system $[Zn(H_2L)Cl_2]$ in DMSO solution (*vide supra*) suggested the presence of dynamic exchange processes, presumably involving the $[Zn(H_2L)Cl_2]$ and $[Zn(H_2L)Cl(OSMe_2)]^+$ species. Addition of an excess of anion shifts the equilibrium to the $[Zn(H_2L)Cl_2]$ form, causing an important deshielding of the NH proton signals.

Fluoride displays a very intricate behavior. Addition of an excess of F^- to a solution of the free receptor H_2L results in the formation at 325 nm of the typical charge-transfer transition from the −NH fragment to the $-NO_2$ group. This is indicative of the double deprotonation of the urea group and formation of the bifluoride anion $[HF_2]^-$ (Figure S2, Supporting Information).[14] Further support for the deprotonation of the receptor comes from the observation of the ^{19}F NMR signal of $[HF_2]^-$ at δ = −144 ppm,[52] and the ^1H NMR signal of the same species at δ = 16.0 ppm.

In the presence of Cu^{II} or Zn^{II}, the metal-based receptor undergoes stepwise deprotonation of the two NH fragments of the urea subunit, events that are signaled by the development of vivid colors. The typical CT band due to the double deprotonation of the urea moiety is clearly observed when the titration is performed at low concentration (10^{-4} M) (Figure S6, Supporting Information). The titration profiles obtained upon F^- addition to $[Cu(H_2L)]^{2+}$ in DMSO solution show four inflection points at Cu^{2+}/F^- molar ratios of 1:1, 1:2, 1:3, and 1:4 (Figure S7, Supporting Information). The first of these processes involves the interaction of a F^- anion with the urea group via hydrogen-bonding. Addition of a second equivalent of anion provokes the monodeprotonation of the urea group. The third equivalent of added anion interacts with the urea NH group via hydrogen-bonding, while addition of a fourth equivalent promotes the deprotonation of the second urea NH group. The double deprotonation of ureas by F^- with concomitant formation of $[HF_2]^-$ has been observed previously.[14e] Deprotonation of the receptor is again confirmed by the observation of the ^{19}F NMR signal of $[HF_2]^-$ at δ = −144 ppm and the ^1H NMR signal of the same species at δ = 16.0 ppm in the Zn^{II} analogue. The $[HF_2]^-$ species is not interacting with the deprotonated metal-receptor, as demonstrated by ^1H DOSY measurements, which were recorded in the presence of 5 equiv of F^- (Figure S9, Supporting Information). These studies provided a diffusion coefficient D = 7.96 × 10^{-10} $m^2 \cdot s^{-1}$ for $[HF_2]^-$, which gives a hydrodynamic radius r_H = 1.29 Å using the Stokes−Einstein equation. As expected due to its larger hydrodynamic radius, the $[Zn(HL)(OSMe_2)]^+$ gives a considerably lower diffusion coefficient (D = 2.17 × 10^{-10} $m^2 \cdot s^{-1}$).

Association Constants. The analysis of the spectrophotometric titrations described above allowed us to calculate the association constants for the interaction of the different anions with the Cu^{II} complex (Table 5). The log K_{11} values obtained for the different anions follow the expected order: $MeCO_2^- \sim Cl^- > NO_2^- > H_2PO_4^- \sim Br^- > HSO_4^- > NO_3^-$. In the case of $MeCO_2^-$ and Cl^-, the steep curvature of the titration profiles indicates especially high equilibrium constants (log K_{11} > 7). In particular, the p parameter was found to be close to 1.0 in both cases (p = [complex concentration]/[maximum possible complex concentration]), a condition that does not permit the determination of a reliable equilibrium constant.[53] On the opposite side of this series of ligands is NO_3^-, which provides a weak binding to $[Cu(H_2L)]^{2+}$; a value of logK_{11} < 2 can be estimated from the titration data.

It is clear that the observed sequence of anion affinity does not parallel the sequence in solvation terms. For instance, small anions such as Cl^-, with a relatively high charge to radius ratio, should be highly solvated, and the endothermic desolvation term should disfavor binding to the metal ion.[54] The association constant log K_{11} determined for Cl^- is higher than that with Br^-, a fact that is in line with the thermodynamic

dx.doi.org/10.1021/ic402855r | Inorg. Chem. 2014, 53, 2554−2568

stability often observed for metal-halide complexes derived from the direct charge−charge interaction with the metal ion,[55] even if this is not a general rule. In both cases, a cooperative effect between the coordinatively unsaturated metal ion and the urea fragment, involved in a bifurcated hydrogen-bonding interaction, reinforces the binding of halides to the metal ion. However, the particularly high association constant observed for Cl^- is probably related to the better hydrogen-bonding acceptor properties of this anion that could further stabilize chloride compared to bromide.[8e]

The observed binding affinity toward the different anions is probably primarily related to the strength of the metal−anion interaction, but steric effects derived from the cooperative hydrogen-bonding interactions probably also play an important role. The especially high affinity constants of NO_2^- and $MeCO_2^-$ can also be related to their relatively low steric requirements and their ability to act as bidentate chelate ligands. The lower log K_{11} value of the adduct with NO_2^- is in line with the lower partial charge of its oxygen atoms in comparison to those of acetate (the atomic polar tensor (APT) charges of the oxygen atoms of NO_2^- and $MeCO_2^-$ calculated at the TPSSh/6-311+G(d,p) level in DMSO solution are −1.00 and −1.27, respectively). The highest affinity toward the tetrahedral anions $H_2PO_4^-$ and HSO_4^- compared with NO_3^- is also probably in line with the APT charges on the oxygen atoms of these oxoanions ($H_2PO_4^-$, −1.25; HSO_4^-, −1.19; NO_3^-, −0.99 at the TPSSh/6-311+G(d,p) level in DMSO solution) and the cooperative effect evidenced in the solid state for the adduct with SO_4^{2-}, where a N-coordination type of the urea fragment is observed. Such a cooperative effect likely prevents the coordination of a second HSO_4^- anion, and as a result the formation of a five-coordinate species with a "bent propeller" conformation is not observed.

CONCLUSIONS

A series of metal complexes with the tripodal ditopic ligand H_2L containing a dpa unit for cation binding and a urea motif for anion recognition have been prepared and characterized. The analysis of the X-ray molecular structures of Cu^{II} and Zn^{II} complexes derived from H_2L indicates a different behavior of the urea moiety when the receptor interacts with different anions. The solid state structure of the Cu^{II} complex with SO_4^{2-} shows a cooperative binding involving simultaneous coordination of the anion to the metal ion and to the urea subunit through two directional hydrogen−bonding interactions. A similar situation is observed in the Zn^{II} complex with Cl^-, but only one of the coordinated anions interacts with the urea fragment in a bifurcated mode. On the contrary, for anions such as NO_3^- and $PhCO_2^-$, two independent and non-cooperative interactions are observed. On one side, the first anion interacts only with the coordinatively unsaturated metal ion, while the second anion is involved in a directional hydrogen-bonding interaction with the urea group, which is projected away from the metal center.

Spectrophotometric titrations carried out for the $[Cu(H_2L)(OSMe_2)_2]^{2+}$ complex and ^1H NMR experiments on the Zn^{II} analogue indicate that in DMSO solution all the investigated anions bind to the coordinatively unsaturated metal ion. Addition of HSO_4^- results in the formation of 1:1 species, presumably due to the presence of a cooperative binding between the metal center and the urea moiety. However, for anions such as Cl^-, NO_2^-, $H_2PO_4^-$, and Br^- the anion excess provokes the formation of 1:2 (metal/anion) species in which only one anion may interact with the urea group through hydrogen bonds. The X-ray structure of the complex with copper sulfate and DFT calculations performed in DMSO solution point to an unexpected N-coordination mode of the urea group to the metal ion in the absence of coordinating anions. The N-coordination of the urea unit enhances its acidity with respect to the free receptor, so that addition of basic anions such as $MeCO_2^-$, $PhCO_2^-$, and F^- promotes the deprotonation of this group. The binding affinity sequence of the different anions to $[Cu(H_2L)(OSMe_2)_2]^{2+}$ follows the following trend: $MeCO_2^- \sim Cl^- > NO_2^- > H_2PO_4^- \sim Br^- > HSO_4^- > NO_3^-$, where a cooperative bifurcated hydrogen-bonding interaction with halides seems to reinforce their binding to the metal ion. This complex has a certain degree of preorganization for the recognition of tetrahedral oxoanions over trigonal planar ones. Indeed, the orientation of the coordinated urea unit allows tetrahedral anions to interact simultaneously with the coordinatively unsaturated metal center and the urea group through directional hydrogen bonds. Current efforts are focused on the design of more sophisticated receptors capable of enhancing the selectivity toward tetrahedral anions in aqueous media for selective metal salt extraction.

ASSOCIATED CONTENT

Supporting Information

X-ray crystallographic files in CIF format for Cu·L·NO_3, Cu·L·SO_4, Cu·L·Bz, and Zn·L·Cl and optimized Cartesian coordinates (Å) of the complexes investigated in this work, main geometrical parameters of the minimum-energy conformations calculated at the (TPSSh/SVP) level, and UV/vis spectra showing the formation of the Cu^{II} complexes. This material is available free of charge via the Internet at http://pubs.acs.org.

AUTHOR INFORMATION

Corresponding Author

*E-mail: david.esteban@udc.es.

Notes

The authors declare no competing financial interest.

ACKNOWLEDGMENTS

The authors thank Xunta de Galicia (EM 2012/088) and (CN 2012/011) for generous financial support and Centro de Supercomputación de Galicia (CESGA) for providing the computer facilities. I.C.-B. thanks Ministerio de Educación y Ciencia (FPU program) for a predoctoral fellowship.

REFERENCES

(1) (a) Caltagirone, C.; Gale, P. A. *Chem. Soc. Rev.* **2009**, *38*, 520−563. (b) Gale, P. A. *Chem. Soc. Rev.* **2010**, *39*, 3746−3771. (c) Wenzel, M.; Hiscock, J. R.; Gale, P. A. *Chem. Soc. Rev.* **2012**, *41*, 480−520. (d) Moyer, B. A.; Custelcean, R.; Hay, B. P.; Sessler, J. L.; Bowman-James, K.; Day, V. W.; Kang, S.-O. *Inorg. Chem.* **2013**, *52*, 3473−3490. (e) Haridas, V.; Sahu, S.; Kumar, P. P. P.; Sapala, A. R. *RSC Adv.* **2012**, *2*, 12594−12605. (f) Chang, J. Y.-C.; Parsons, S.; Plieger, P. G.; Tasker, P. A. *J. Inclusion Phenom. Marocryclic Chem.* **2011**, *71*, 529−536.

(2) (a) *Anion Coordination Chemistry*; Bowman-James, K., Bianchi, A., Garcia-España, E., Eds.; Wiley-VCH: New York, 2011; Chapters 1−2. (b) Beer, P. D.; Gale, P. A. *Angew. Chem., Int. Ed.* **2001**, *40*, 486−516.

(3) *Anion Coordination Chemistry*; Bowman-James, K., Bianchi, A., Garcia-España, E., Eds.; Wiley-VCH: New York, 2011; Chapter 3.

(4) (a) Bowman-James, K. *Acc. Chem. Res.* **2005**, *38*, 671−678. (b) Kang, S. O.; Hossain, Md. A.; Bowman-James, K. *Coord. Chem. Rev.* **2006**, *250*, 3038−3052. (c) Fowler, C. J.; Haverlock, J.; Moyer, B. A.; Schriver, J. A.; Gross, D. E.; Marquez, M.; Sessler, J. L.; Hossain, Md. A.; Bowman-James, K. *J. Am. Chem. Soc.* **2008**, *130*, 14386−14387.
(5) Cavallo, G.; Metrangolo, P.; Pilati, T.; Resnati, G.; Sansotera, M.; Terraneo, G. *Chem. Soc. Rev.* **2010**, *39*, 3772−3783.
(6) (a) Custelcean, R. *Top. Curr. Chem.* **2012**, *322*, 193−216. (b) Ballester, P. *Chem. Soc. Rev.* **2010**, *39*, 3810−3830. (c) Frischmann, P. D.; MacLachlan, M. J. *Chem. Soc. Rev.* **2013**, *42*, 871−890.
(7) (a) Fabbrizzi, L.; Poggi, A. *Chem Soc. Rev.* **2013**, *42*, 1681. (b) Amendola, V.; Fabbrizzi, L. *Chem. Commun.* **2009**, 513−531. (c) O'Neil, E. J.; Smith, B. D. *Coord. Chem. Rev.* **2006**, *250*, 3068−3080. (c) Verdejo, B.; Aguilar, J.; Domenech, A.; Miranda, C.; Navarro, P.; Jimenez, H. R.; Soriano, C.; Garcia-España, E. *Chem. Commun.* **2005**, 3086−3088.
(8) (a) Kim, S. K.; Sessler, J. L. *Chem Soc. Rev.* **2010**, *39*, 3784−3809. (b) McConnell, A. J.; Beer, P. D. *Angew. Chem., Int. Ed.* **2012**, *51*, 5052−5061. (c) Dalla Cort, A. In *Supramolecular Chemistry: From Molecules to Nanomaterials*; Gale, P. A., Steed, J. W., Eds.; Wiley & Sons, Ltd.: Hoboken, NJ, 2011; Chapter 3; pp 1281−1308. (d) Lang, K.; Park, J.; Hong, S. *Angew. Chem., Int. Ed.* **2012**, *51*, 1620−1624. (e) Ambrosi, G.; Formica, M.; Fusi, V.; Giorgi, L.; Macedi, E.; Micheloni, M.; Paoli, P.; Pontellini, R.; Rossi, P. *Chem.—Eur. J.* **2011**, *17*, 1670−1682.
(9) (a) Ngo, H. T.; Liu, X.; Jolliffe, K. A. *Chem. Soc. Rev.* **2012**, *41*, 4928−4965. (b) Humphreys, K. J.; Karlin, K. D.; Rokita, S. E. *J. Am. Chem. Soc.* **2002**, *124*, 8055−8066. (c) Hernandez-Gil, J.; Ferrer, S.; Salvador, E.; Calvo, J.; Garcia-España, E.; Mareque-Rivas, J. C. *Chem. Commun.* **2013**, *49*, 3655. (d) Belousoff, M. J.; Tjioe, L.; Graham, B.; Spiccia, L. *Inorg. Chem.* **2008**, 8641−8651.
(10) (a) Glerup, J.; Goodson, P. A.; Hodgson, D. J.; Michelsen, K.; Nielsen, K. M.; Weihe, H. *Inorg. Chem.* **1992**, *31*, 4611−4616. (b) Yashiro, M.; Kaneiwa, H.; Onaka, K.; Komiyama, M. *Dalton Trans.* **2004**, 605−610. (c) Palaniandavar, M.; Butcher, R. J.; Addison, A. W. *Inorg. Chem.* **1996**, *35*, 467−471.
(11) (a) O'Neil, E. J.; Smith, B. D. *Coord. Chem. Rev.* **2006**, *250*, 3068−3080. (b) Milaeva, E. R.; Shpakovsky, D. B.; Gracheva, Y. A.; Orlova, S. I.; Maduar, V. V.; Tarasevich, B. N.; Leleshonkova, N. N.; Dubova, L. G.; Schevtsova, E. F. *Dalton Trans.* **2013**, *42*, 6817−6828. (c) Fischmann, A. J.; Forsyth, C. M.; Spiccia, L. *Inorg. Chem.* **2008**, *47*, 10565−10574. (d) Tjioe, L.; Joshi, T.; Brugger, J.; Graham, B.; Spiccia, L. *Inorg. Chem.* **2011**, *50*, 621−635.
(12) (a) Kim, S. Y.; Hong, J. I. *Bull. Korean Chem. Soc.* **2010**, *31*, 716−719. (b) Chen, Z.-H.; Lu, Y.; He, Y.-B.; Huang, X.-H. *Sens. Actuators, B: Chem.* **2010**, *149*, 407−412. (c) Kim, S. Y.; Li, D. H.; Hong, J.-I.; Yoon, J. *Acc. Chem. Res.* **2009**, *42*, 23−31. (d) Amendola, V.; Bergamaschi, G.; Boiocchi, M.; Fabbrizzi, L.; Mosca, L. *J. Am. Chem. Soc.* **2013**, *135*, 6345−6355. (e) Veale, E. B.; Tocci, G. M.; Pfeffer, F. M.; Kruger, P. E.; Gunnlaugsson, T. *Org. Biomol. Chem.* **2009**, *7*, 3447−3454. (f) Ghosh, K.; Sarkar, T. *J. Inclusion Phenom. Macrocyclic Chem.* **2011**, *71*, 243−248.
(13) (a) Amendola, V.; Fabbrizzi, L.; Mosca, L.; Schmidtchen, F. P. *Chem.—Eur. J.* **2011**, *17*, 5972−5981. (b) Baggi, G.; Boiocchi, M.; Ciarrocchi, C.; Fabbrizzi, L. *Inorg. Chem.* **2013**, *52*, 5273−5283. (c) Amendola, V.; Esteban-Gomez, D.; Fabbrizzi, L.; Licchelli, M. *Acc. Chem. Res.* **2006**, *39*, 343−353. (d) Amendola, V.; Bonizzoni, M.; Esteban-Gomez, D.; Fabbrizzi, L.; Licchelli, M.; Sancenon, F.; Taglietti, A. *Coord. Chem. Rev.* **2006**, *250*, 1451−1470.
(14) (a) Amendola, V.; Fabbrizzi, L.; Mosca, L. *Chem. Soc. Rev.* **2010**, *39*, 3889−3915. (b) Boiocchi, M.; Del Boca, L.; Gomez, D. E.; Fabbrizzi, L.; Licchelli, M.; Monzani, E. *J. Am. Chem. Soc.* **2004**, *126*, 16507−16514. (c) Boiocchi, M.; Del Boca, L.; Esteban-Gomez, D.; Fabbrizzi, L.; Licchelli, M.; Monzani, E. *Chem.—Eur. J.* **2005**, *11*, 3097−3104. (d) dos Santos, C. M. G.; McCabe, T.; Watson, G. W.; Kruger, P.; Gunnlaugsson, T. *J. Org. Chem.* **2008**, *73*, 9235−9244. (e) Esteban-Gomez, D.; Fabbrizzi, L.; Licchelli, M. *J. Org. Chem.* **2005**, *70*, 5717−5720.
(15) (a) Amendola, V.; Boiocchi, M.; Colasson, B.; Fabbrizzi, L. *Inorg. Chem.* **2006**, *45*, 6138−6147. (b) Fisher, M. G.; Gale, P. A.; Light, M. E.; Loeb, S. J. *Chem. Commun.* **2008**, 5695−5697. (c) Amendola, V.; Boiocchi, M.; Colasson, B.; Fabbrizzi, L.; Rodriguez-Douton, M.-J.; Ugozzoli, F. *Angew. Chem., Int. Ed.* **2006**, *45*, 6920−6924. (d) Custelcean, R.; Bosano, J.; Bonnesen, P. V.; Kertesz, V.; Hay, B. P. *Angew. Chem., Int. Ed.* **2009**, *48*, 4025−4029.
(16) (a) Romanski, J.; Piatek, P. *Chem. Commun.* **2012**, *48*, 11346−11348. (b) Ballistreri, F. P.; Notti, A.; Pappalardo, S.; Parisi, M. F.; Pisagatti, I. *Org. Lett.* **2003**, *5*, 1072−1074. (c) Garozzo, D.; Gattuso, G.; Notti, A.; Pappalardo, A.; Pappalardo, S.; Parisi, M. F.; Perez, M.; Pisagatti, I. *Angew. Chem., Int. Ed.* **2005**, *45*, 4892−4896. (d) Glenny, M. W.; Blake, A. J.; Wilson, C.; Schröder, M. *Dalton Trans.* **2003**, 1941−1951.
(17) (a) Piatek, P. *Chem. Commun.* **2011**, *47*, 4745−4747. (b) He, X.; Yam, V. W.-W. *Inorg. Chem.* **2010**, *49*, 2273−2279. (c) Chen, Y.; Wang, D.-X.; Huang, Z.-T.; Wang, M.-X. *Chem. Commun.* **2011**, *47*, 8112−8114.
(18) (a) Amendola, V.; Esteban-Gomez, D.; Fabbrizzi, L.; Licchelli, M.; Monzani, E.; Sancenon, F. *Inorg. Chem.* **2005**, *44*, 8690−8698. (b) Allevi, M.; Bonizzoni, M.; Fabbrizzi, L. *Chem.—Eur. J.* **2007**, *13*, 3787−3795.
(19) Gans, P.; Sabatini, A.; Vacca, A. *Talanta* **1996**, *43*, 1739−1753.
(20) SADABS, Bruker-AXS, Version 1; Bruker AXS Inc.: Madison, WI, 2004.
(21) Sheldrick, G. M. *Acta Crystallogr.* **2008**, *A64*, 112−122.
(22) Farrugia, L. J. *J. Appl. Crystallogr.* **1999**, *32*, 837−838.
(23) DIRDIF99. Beurskensaaa, P. T.; Beurskens, G.; de Gelder, R.; Garcia-Granda, S.; Gould, R. O.; Israel, R.; Smits, J. M. M. The DIRDIF-99 program system, Technical Report of the Crystallography Laboratory; University of Nijmegen: The Netherlands, 1999.
(24) SQUEEZE. Van der Sluis, P.; Spek, A. L. *Acta Crystallogr.* **1990**, *A46*, 194−201.
(25) *Gaussian 09*, Revision A.01; Frisch, M. J.; Trucks, G. W.; Schlegel, H. B.; Scuseria, G. E.; Robb, M. A.; Cheeseman, J. R.; Scalmani, G.; Barone, V.; Mennucci, B.; Petersson, G. A.; Nakatsuji, H.; Caricato, M.; Li, X.; Hratchian, H. P.; Izmaylov, A. F.; Bloino, J.; Zheng, G.; Sonnenberg, J. L.; Hada, M.; Ehara, M.; Toyota, K.; Fukuda, R.; Hasegawa, J.; Ishida, M.; Nakajima, T.; Honda, Y.; Kitao, O.; Nakai, H.; Vreven, T.; Montgomery, Jr., J. A.; Peralta, J. E.; Ogliaro, F.; Bearpark, M.; Heyd, J. J.; Brothers, E.; Kudin, K. N.; Staroverov, V. N.; Kobayashi, R.; Normand, J.; Raghavachari, K.; Rendell, A.; Burant, J. C.; Iyengar, S. S.; Tomasi, J.; Cossi, M.; Rega, N.; Millam, N. J.; Klene, M.; Knox, J. E.; Cross, J. B.; Bakken, V.; Adamo, C.; Jaramillo, J.; Gomperts, R.; Stratmann, R. E.; Yazyev, O.; Austin, A. J.; Cammi, R.; Pomelli, C.; Ochterski, J. W.; Martin, R. L.; Morokuma, K.; Zakrzewski, V. G.; Voth, G. A.; Salvador, P.; Dannenberg, J. J.; Dapprich, S.; Daniels, A. D.; Farkas, Ö.; Foresman, J. B.; Ortiz, J. V.; Cioslowski, J.; Fox, D. J. Gaussian, Inc.: Wallingford, CT, 2009.
(26) Tao, J. M.; Perdew, J. P.; Staroverov, V. N.; Scuseria, G. E. *Phys. Rev. Lett.* **2003**, *91*, 146401.
(27) Schaefer, A.; Horn, H.; Ahlrichs, R. *J. Chem. Phys.* **1992**, *97*, 2571−2577.
(28) Stanton, J. F.; Gauss, J. *Adv. Chem. Phys.* **2003**, *125*, 101−146.
(29) Tomasi, J.; Mennucci, B.; Cammi, R. *Chem. Rev.* **2005**, *105*, 2999−3093.
(30) (a) Matsumura, M.; Tanatani, A.; Azumaya, I.; Masu, H.; Hashizume, D.; Kagechika, H.; Muranaka, A.; Uchiyama, M. *Chem. Commun.* **2013**, *49*, 2290−2292. (b) Vidaluc, J.-L.; Calmel, F.; Bigg, D.; Carilla, E.; Stenger, A.; Chopin, P.; Briley, M. *J. Med. Chem.* **1994**, *37*, 689−695.
(31) Yadav, L. D. S. *Organic Spectroscopy*; Kluwer Academic Publishers: Dordrecht, The Netherlands, 2005; p 42.
(32) Elleb, M.; Meullemeestre, J.; Schwing-Weill, M.-J.; Vierling, F. *Inorg. Chem.* **1982**, *21*, 1477−1483.
(33) Addison, A. W.; Nageswara-Rao, T.; Reedijk, J.; van Rijn, J.; Verschoor, G. C. *J. Chem. Soc., Dalton Trans.* **1984**, 1349−1356.

(34) (a) Allen, C. S.; Chuang, C.-L.; Cornebise, M.; Canary, J. W. *Inorg. Chim. Acta* **1995**, *239*, 29−37. (b) Canary, J. W.; Allen, C. S.; Castagnetto, J. M.; Chiu, Y.-H.; Toscano, P. J.; Wang, Y. *Inorg. Chem.* **1998**, *37*, 6255−6262. (c) Abufarag, A.; Vahrenkamp, H. *Inorg. Chem.* **1995**, *34*, 2207−2216. (d) Sun, B.-W.; Wang, Z.-M.; Gao, S. *Inorg. Chem. Commun.* **2001**, *4*, 79−81. (e) Kwon, J. E.; Lee, S.; You, Y.; Baek, K.-H.; Ohkubo, K.; Cho, J.; Fukuzumi, S.; Shin, I.; Park, S. Y.; Nam, W. *Inorg. Chem.* **2012**, *51*, 8760−8774. (f) Makowska-Grzyska, M. M.; Szajna, E.; Shipley, C.; Arif, A. M.; Mitchell, M. H.; Halfen, J. A.; Berreau, L. M. *Inorg. Chem.* **2003**, *42*, 7472−7488. (g) Mikata, Y.; Fuji, S.; Naemura, M.; Takahashi, K.; Noguchi, Y. *Dalton Trans.* **2009**, 10305−10310.

(35) Janiak, C. *J. Chem. Soc., Dalton Trans.* **2000**, 3885−3896.

(36) Desiraju, G. R.; Steiner, T. *The Weak Hydrogen Bond*; Oxford University Press: 1999; Chapter 3.

(37) Aullon, G.; Bellamy, D.; Brammer, L.; Bruton, E. A.; Orpen, A. G. *Chem. Commun.* **1998**, 653−654.

(38) Yap, G. P. A.; Rheingold, A. L.; Das, P.; Crabtree, R. H. *Inorg. Chem.* **1995**, *34*, 3474−3476.

(39) (a) Bondi, A. *J. Phys. Chem.* **1964**, *68*, 441−451. (b) Metrangolo, P.; Meyer, F.; Pilati, T.; Resnati, G.; Terraneo, G. *Angew. Chem., Int. Ed.* **2008**, *47*, 6114−6127.

(40) (a) Jahn, H.; Teller, E. *Proc. R. Soc. London, Ser. A* **1937**, *161*, 220. (b) Halcrow, M. A. *Chem. Soc. Rev.* **2013**, *42*, 1784−1795.

(41) Hay, B. P.; Gutowski, M.; Dixon, D. A.; Garza, J.; Vargas, R.; Moyer, B. A. *J. Am. Chem. Soc.* **2004**, *126*, 7925−7934.

(42) (a) Jeffrey, G. A. *An Introduction to Hydrogen Bonding*; Truhlar, D. G., Ed.; Oxford University Press: Oxford, 1997. (b) Steiner, T. *Angew. Chem., Int. Ed.* **2002**, *41*, 48−76. (c) Caltagirone, C.; Bates, G. W.; Gale, P. A.; Light, M. E. *Chem. Commun.* **2008**, 61−63.

(43) Hay, B. P.; Dixon, D. A.; Bryan, J. C.; Moyer, B. A. *J. Am. Chem. Soc.* **2002**, *124*, 182−183.

(44) Regueiro-Figueroa, M.; Djanashvili, K.; Esteban-Gomez, D.; de Blas, A.; Platas-Iglesias, C.; Rodriguez-Blas, T. *Eur. J. Org. Chem.* **2010**, 3237−3248.

(45) Puchta, R.; Hommes, E.; van, E.; Meier, R.; van Eldik, R. *Dalton Trans.* **2006**, 3392−3395.

(46) Maslak, P.; Sczepanski, J. J.; Parvez, M. *J. Am. Chem. Soc.* **1991**, *113*, 1062−1063.

(47) (a) Niklas, N.; Heinemann, F. W.; Hampel, F.; Clark, T.; Alsfasser, R. *Inorg. Chem.* **2004**, *43*, 4663−4673. (b) Niklas, N.; Hampel, F.; Liehr, G.; Zahl, A.; Alsfasser, R. *Chem.—Eur. J.* **2001**, *7*, 5135−5142.

(48) Choi, K.-Y.; Jeon, Y.-M.; Ryu, H.; Oh, J.-J.; Lim, H.-H.; Kim, M.-W. *Polyhedron* **2004**, *23*, 903−911.

(49) (a) Murakami, T.; Takei, T.; Ishikawa, Y. *Polyhedron* **1997**, *16*, 89−93. (b) Su, C. C.; Lu, W. S.; Hui, T. Y.; Chang, T. Y.; Wang, S. L.; Liao, F. L. *Polyhedron* **1993**, *12*, 2249−2259.

(50) Bordwell, F. G. *Acc. Chem. Res.* **1988**, *21*, 456−463.

(51) Jakab, G.; Tancon, C.; Zhang, Z.; Lippert, K.-M.; Schreiner, P. R. *Org. Lett.* **2012**, *14*, 1724−1727.

(52) (a) Goursaud, M.; De Bernardin, P.; Dalla Cort, A.; Bartik, K.; Bruylants, G. *Eur. J. Org. Chem.* **2012**, 3570−3574. (b) Kang, S. O.; Powell, D.; Day, V. W.; Bowman-James, K. *Angew. Chem., Int. Ed.* **2006**, *45*, 1921−1925.

(53) Wilcox, C. S. *Frontiers in Supramolecular Chemistry and Photochemistry*; VCH Verlagsgesellschaft: Weinheim, 1991; pp 123−143.

(54) Boiocchi, M.; Fabbrizzi, L.; Foti, F.; Poggi, A. *C. R. Chim.* **2005**, *8*, 1519−1526.

(55) Ambrosi, G.; Formica, M.; Fusi, V.; Giorgi, L.; Guerri, A.; Micheloni, M.; Paoli, P.; Pontellini, R.; Rossi, P. *Chem.—Eur. J.* **2007**, *13*, 702−712.